

Original

THE USE OF CARBON DIOXIDE AS AN ENHANCED RECOVERY AGENT FOR INCREASING HEAVY OIL PRODUCTION

D. Brant Bennion and F. Brent Thomas
Hycal Energy Research Laboratories Ltd.

Prepared for presentation at the Joint Canada/Romania Heavy Oil Symposium
March 7-13, 1993 at Sinia, Romania.

ABSTRACT

Carbon dioxide (CO₂) exhibits extremely high solubility at relatively low pressures in heavy oil. Dissolution of CO₂ in heavy oils reduces viscosity and increases swelling and internal drive energy, both of which aid in the recovery of additional heavy oil. This paper presents a summary of a wide range of laboratory and coreflood tests conducted on three different live oils (i.e., oil initially containing solution gas) varying from 9.6 to 15° API. These tests were used to investigate the use of CO₂ and its effect on parameters such as viscosity, density, solubility and swelling as a function of pressure at temperatures from 20-175° C. The test results indicate substantial reductions in viscosity and increases in swelling and gas solubility when the oils are contacted with CO₂.

INTRODUCTION

Carbon dioxide (CO₂) will perform a significant role in enhanced oil recovery (EOR) as the price of crude oil increases. Carbon dioxide can be obtained naturally in some parts of the world and is a by-product of some refining and processing operations. As the price of crude oil increases, the economics of obtaining CO₂ from these refining and processing operations may improve, thus making significant quantities of CO₂ economically available. The main use of CO₂ for EOR has been in light crude oil reservoirs, but several immiscible CO₂ displacements are presently being conducted in reservoirs containing heavier oils. Some of these pilots have shown good production response to the injected CO₂.

Carbon dioxide has also been used as an additive with steam and is generated in-situ in an oxygen fireflood. Little information is available in the literature on the behavior of CO₂ and heavy oils containing solution gas. Most of the available data has been presented for CO₂ and dead reservoir crude oils.

The objectives of this study were to measure viscosity, solubility, swelling and density data and to perform corefloods using three heavy oils and CO₂. The collected data was to be used to better understand the mechanism of immiscible CO₂ displacement and to obtain correlations which could be used to predict fluid transport properties.

The three oils analyzed were obtained from three different Canadian heavy oil reservoirs. These oils were selected to cover a range of API gravities from 9.6° to 15.0° API. This paper is divided into the following sections:

1. Description of CO₂ phase behavior properties.
2. Oil property measurements
 - a) procedures
 - b) experimental equipment
 - c) test results
 - d) numerical correlations
3. Coreflow tests
 - a) procedures
 - b) experimental equipment
 - c) test results

CO₂ PHASE BEHAVIOR PROPERTIES

Carbon dioxide (CO₂) is a clear colorless gas. A summary of CO₂ properties is contained in Appendix "A" of the paper. Carbon dioxide is a diatomic molecule and exhibits extremely high solubility in both aqueous and hydrocarbon solutions. This high solubility contributes greatly to the potential use of CO₂ as an enhanced oil recovery agent.

Figures 1 and 2 illustrate a typical pressure-composition and pressure-temperature diagram for a CO₂-hydrocarbon system. The configuration of the phase envelope and presence and size of the three phase envelope depends on the type of oil and on the system temperature under consideration. For most CO₂-hydrocarbon systems, true first contact miscibility cannot be established due to the high pressure required in order to exceed the cricondenbar on the pressure-temperature diagram. For lighter oil systems, at relatively high (> 17 MPa) pressures, vaporizing type multicontact miscibility, which is an extremely efficient process, can often be established with CO₂. For heavier oils or severely depleted reservoirs, where reservoir pressure is very low and cannot be increased due to economic or technical reasons, CO₂ can also be used effectively in an immiscible mode.

Due to its relatively low equilibrium ratio (k factor) in relation to other volatile gaseous components (such as nitrogen or methane), CO₂ tends to preferentially be retained in the liquid hydrocarbon phase. Carbon dioxide also has the advantage of being an inert, non flammable gas which is non-toxic to humans and can be easily transported (and even injected) in a liquid form at relatively low pressures. It also has a much greater viscosity and higher density than conventional miscible or immiscible gas injection agents which tends to reduce problems associated with gravity override and viscous fingering effects.

Potential disadvantages of CO₂ include limited availability in some areas of the world, corrosion problems associated with the use of CO₂ in saline brine environments (particularly in the presence of dissolved oxygen) and a propensity for some oil systems to precipitate asphaltenes and other high molecular weight insoluble solids when contacted by CO₂. Sufficient design and experimental work conducted prior to the implementation of a CO₂ project can generally eliminate many uncertainties and reduce future operational problems by diagnosing the potential for certain problems prior to the implementation of the field design and allowing for the constraints imposed by these potential problems in the initial design strategy.

Since heavy oil immiscible CO₂ projects, which are the subject of this paper, rely upon the effect of CO₂ dissolving into solution into the gas to increase recovery, a proper understanding of how CO₂ contact alters the transport properties of gas saturated heavy crude oils is essential. Carbon dioxide can enhance the recovery of heavy oils in the following manner:

1. Viscosity Reduction - As CO₂ dissolves into the heavy oil, viscosity is reduced. This is due to the much lower viscosity of CO₂ in comparison to the heavy oil.
2. Increase in Oil Swelling - As CO₂ dissolves into solution, the oil formation volume factor increases expanding the apparent volume of the oil in place and enhancing drive energy.
3. Increased Solubility - The CO₂ has a much greater solubility than conventional gas and one can obtain much higher gas-oil ratios than with gases such as solution gas, methane or nitrogen. This higher dissolved gas content increases the natural drive energy available to produce the reservoir.

Examination of Figure 1 indicates that at a given temperature, one can see a transition to liquid-liquid equilibria at higher pressures. This phenomenon is associated with a change in mass transfer mechanism - solubility of CO₂ in hydrocarbon liquid at lower CO₂ concentrations, which requires less pressure, as opposed to extraction of hydrocarbon components into the upper phase as the CO₂ concentration increases. Accompanying this change is the bubblepoint to dewpoint transition. For heavier oils or for lower temperatures (less than 0 to 100° C), in order to extract all compounds to create a single phase, which would then correspond to a vapor, the pressure must

increase very rapidly. This continues to increase rapidly since extracted components alter the extraction capability of the upper phase CO₂. For lighter oils, the upper phase can extract the oil much more readily and thus the P-X response usually is flatter than the heavy oil response in Figure 1.

OIL PROPERTY MEASUREMENTS

Procedures

Fluid property measurements as a function of CO₂ saturation pressure and temperature were conducted on the 9.6°, 12.4° and 15° API oils. These measurements included:

1. Viscosity
2. Density
3. Solubility
4. Swelling.
5. Saturation Pressure

The tests were conducted at the appropriate respective reservoir temperature for each oil and at temperatures of 100° C and 175° C for each of the oils. At each temperature for each oil, measurements were conducted on the initial live oil and on the CO₂-saturated oil at four or five successively higher CO₂ saturation levels. A total of 47 experimental points were determined in the study: 16 for the 15° API oil; 15 for the 12.4° API oil; and 16 for the 9.6° API oil. The procedure for the measurement of viscosity, density and solubility follows in the experimental equipment discussion. The procedures for measuring swelling and saturation pressure will now be discussed, as well as the procedure for oil and CO₂ addition and the oil recombination.

Oil Recombination

The initial oil recombination for the 9.6°, 12.4°, and 15° API oils was performed by charging a specified amount of dead oil into a blind high pressure stainless steel cylinder. The oil was then exposed to solution gas at the specified bubble point pressure and reservoir temperature and mechanically agitated for 96 hours to mix the two phases. Once the recombination was complete, the oil was pressured to well above the bubble point and a pressure-volume test was conducted to check the bubble point. The initial oil solution G.O.R. was also measured once a satisfactory saturation pressure had been obtained.

CO₂ ADDITION PROCEDURE

For each CO₂ saturation point, a specified volume of oil was charged into the piston at 7.0 MPa (1000 psig) and heated to test temperature. A specified volume of carbon dioxide was injected at pressure into the piston. System pressure was then elevated to 20.68 MPa (3000 psig), and the oven was allowed to rotate for 24 hours to ensure that the sample was well mixed and homogeneous. A pressure volume test was conducted to determine the saturation pressure of the live oil/CO₂ mixture. Once this had been completed, the pressure was increased to 20.68 Mpa (3000 psig) for an additional 20 hours to ensure that all of the evolved gas returned into solution.

Swelling Measurement

Swelling, as defined in this paper, was the increase in saturated liquid phase volume compared to the initial reference volume at temperature and saturation pressure caused by the addition of CO₂. Swelling was measured by noting the single-phase saturated liquid volume at the bubble point, and dividing this into the live oil volume (including CO₂) at the same temperature and the new saturation pressure.

Bubble Point Determination

The bubble point pressure was determined by conducting an isothermal flash expansion test; sample volume was increased in a constant composition expansion test. The stable pressure was noted after each volume increase. A plot of pressure vs system volume or incremental volume withdrawn indicated the bubble point. Due to the heavy nature of the oils in the study and the very slow liberation of gas from the oils, particularly at low temperatures, each pressure-volume curve took approximately 72 to 96 hours to accurately determine.

Specific Experimental Procedure for an Individual Test Point

1. Charge system with live oil at well above bubble point pressure.
2. Allow thermal equilibrium to be established (in the elevated temperature points).
3. Add CO₂ (if required), wait for thermal equilibrium in elevated temperature points.
4. Elevate pressure to 20.68 MPa (3000 psig) and rotate oven to mix phases.
5. Conduct pressure-volume test to determine saturation pressure; calculate swelling.
6. Elevate pressure to 20.68 MPa (3000 psig) to remix.
7. Lower pressure to slightly above bubble point (approx. 70 kPa, 10 psig) to ensure single-phase.
8. Measure viscosity.
9. Measure solubility.
10. Measure density.

DESCRIPTION OF EXPERIMENTAL EQUIPMENT USED IN OIL PROPERTY MEASUREMENTS

Figure 3 provides a schematic of the experimental equipment used in the CO₂ heavy oil PVT study. The heart of the apparatus is a specially designed 316 SS piston into which the sample was charged. A piston was used due to problems encountered with heavy oils in visual cells (i.e., oil sticking to the surface of the sightglass, etc.). The piston

body was rated for pressures of up to 69 MPa (10,000 psig) at 175° C.

The piston's internal volume was varied by injecting hydraulic oil into the base of the system which caused the piston shaft to move upwards. The piston was equipped with an upper and lower set of expandable, machined, teflon seals. The piston has been calibrated so that its internal volume, as a function of the linear position of the piston shaft, was known. The piston shaft was connected directly to a linear variable electronic potentiometer which can measure the position of the piston to within 0.01 mm. This facilitated calculation of the internal volume of the sample chamber to within 0.01 cm³. The dead volumes associated with the lines and valving at the top of the piston were also measured and were taken into consideration in the calculations.

The reservoir of hydraulic oil used to move the piston was contained within the oven body so that it was in thermal equilibrium with the test. This negated fluid expansion effects which would have accompanied the transfer of ambient temperature fluids into the hot piston.

Pressure in the visual cell was measured using a 69 MPa (10,000 psig) gauge which was accurate to 0.17 MPa (25 psi). The gauge was calibrated with a dead weight tester prior to starting each test series. An in-line stainless steel isolator prevented the migration of oil or gas into the gauge which could cause erroneous pressure readings.

Viscosity of a live reservoir fluid at a specified pressure and temperature was measured by displacing the fluid at a known constant rate through a stainless steel capillary tube of known length and internal diameter. The displacement and transfer of all fluids during all phases of the test was performed using Ruska type positive displacement pumps. These pumps can inject at rates from 1 cm³ to 240 cm³/hr at pressures of up to 69 MPa (10,000 psig) and are volumetrically accurate to within 0.02 cm³. The viscosity tube was calibrated prior to the test series by displacing several different fluids of known viscosity through the tube at different temperatures and pressures. Poiseuille's law for laminar single-phase flow in a circular cross-section was used to calculate the viscosity of an unknown fluid once the tube had been calibrated. Poiseuille's law is only applicable to Newtonian fluids, but most oils and oil-gas mixtures can be classified as such.

Pressure drop across the viscosity tube was measured using a Validyne Model DP15 pressure transducer. The pressure transducer has a body pressure rating of 27.5 MPa (4000 psig) and can be equipped to accurately measure pressure differentials from 0.138 to 7.0 MPa (20 to 1000 psig) to within 0.25% of the full scale value by the installation of different plates. The plate selection depends upon the approximate expected viscosity of the oil to be analyzed. The transducer outputs directly to a multi-channel digital Validyne terminal which provided an instantaneous display of the pressure differential at any given time. The transducer also outputs to a strip chart recorder which provides a continuous record of the pressure profile across the viscosity

tube and indicates when steady state has been achieved. Two separate viscosity tubes were mounted within the oven in a manifold type arrangement; one had a 1.588 mm (1/16") outside diameter, and the second a 3.175 mm (1/8") outside diameter to facilitate the measurement of a wider range of viscosities. Stainless steel isolators prevented the migration of any oil and gas up into the transducer system which would have caused erroneous pressure readings. The transducer was calibrated prior to the start of each series at test pressure using a dead weight tester to ensure accurate measurement of the pressure differential.

Backpressure was closely controlled during the viscosity measurements using a 316 SS type backpressure valve rated for 20.68 MPa (3000 psi). An intermediate sample bomb containing water was used to collect the oil which in turn displaced the water out through the backpressure valve.

A small high pressure aluminum cylinder was used to determine the density of live oil samples at temperature and pressure. The aluminum construction of the cylinder renders its tare weight low enough to allow weighing it on an electronic balance accurate to 0.001 g. The sample cylinder was initially evacuated and weighed to determine a tare weight. A known volume of live oil was displaced into the sample cylinder at a specified temperature and pressure. The sample cylinder was re-weighed and the total mass of the transferred sample determine. Since the transferred fluid volume was known, the density of the sample could be calculated.

Solubility was determined by flashing the live oil from the density cylinder into an atmospheric Ruska separator. The separator can measure the oil and gas phase volumes to 0.1 cm³. The density cylinder was re-weighed after emptying to account for any residual heavy oil which should be included in the oil phase volume for solubility calculations. The barometric pressure and ambient temperature were recorded at each flash to facilitate the correction of the gas phase volume back to standard conditions of 15.56° C and 101.325 kPa (60° F, 14.696 psia). The oil phase volume was not corrected due to the small temperature and pressure effects associated with low fluid compressibility and thermal expansion. The corrected gas phase volume was used with the measured oil phase volume to calculate the solubility at any given point.

The piston, viscosity tube, isolators and other associated equipment were mounted within a temperature controlled oven. Temperature was regulated using a ERD digital temperature controller accurate to ± 0.5° C. Thermocouples, mounted in the oven, were connected to an external digital display which provided a continuous readout of the internal system temperature. The oven also contained a visual mercury thermometer as a backup to the thermocouple. Twin circulating fans, operating continuously in the oven, eliminated unwanted temperature gradients and ensured an even temperature distribution. The oven was also equipped with radiator housing through which refrigerant could be circulated to maintain a constant temperature during low temperature runs (i.e., 15° C - 20° C).

The oven was mounted on a rotating bracket which allowed the entire apparatus to be rotated through 180°. This arrangement facilitated the mixing of the oil and gas phases in the piston and ensured a homogeneous composition. The oven can be set to rotate on a continuous or timed basis.

Initial dead oil samples were cleaned by ultra high-speed centrifuging (20,000 rpm) at 50° C to remove any residual water or solids. Only cleaned dead oil was recombined with gas to obtain representative results.

TEST RESULTS - OIL PROPERTY MEASUREMENTS

Table 1 provides a summary of the original recombined live oil compositions for the three oils utilized in the study. The following nomenclature was utilized to describe the oils:

- Oil #1 - 15.0° API gravity crude
- Oil #2 - 12.4° API gravity crude
- Oil #3 - 9.6° API gravity crude

Oil #1 was recombined using actual field solution gas. Solution gas was unavailable for oils #2 and #3 so pure methane gas (C₁) was utilized in these recombinations.

Tables 2 - 4 contain the results of the saturation pressure measurements conducted on each oil as a function of temperature and CO₂ concentration. This data has been plotted as Figures 4 to 6.

Table 5 summarizes the transport property measurements (viscosity, density, solubility and swelling) as a function of both temperature and CO₂ concentration for Oil #1. This data has been plotted and appears As Figures 7 - 10.

Table 6 and Figures 11 - 14 and Table 7 and Figures 15 - 18 provide comparable results for Oil #2 and Oil #3 respectively.

Evaluation of these data indicates that:

1. In general, saturation pressure was found to increase with both increases in CO₂ content and temperature (as would be expected). A flattening trend in the saturation pressure vs CO₂ concentration profiles at high mole fractions of CO₂ can possibly be attributed to the presence of liquid-liquid equilibria conditions being established at high CO₂ mole fractions, resulting in effective extraction of the liquid hydrocarbon phase components leading to a one-phase system.
2. Viscosity was reduced dramatically by CO₂ addition, particularly at low (reservoir) temperatures. Examples for the reservoir oils indicated that:

Oil #	Initial Oil Viscosity (mPa.s)	CO ₂ Saturated Oil Viscosity (mPa.s)	% Reduction
1	953	22	97.6%
2	5660	196	96.5%
3	25022	372	98.5%

The magnitude of viscosity reductions which can reasonably be attained in the field may not be as great as this, as CO₂ saturation pressures in the range of 19 mPa were required to achieve these viscosity reductions. If cutoff saturation pressures in the range of 7 - 8 MPa are utilized instead, substantial viscosity reductions are still apparent:

Oil #	Initial Oil Viscosity (mPa.s)	CO ₂ Saturated Oil Viscosity (mPa.s) at ≈ 8 MPa	% Reduction
1	953	171	82.1%
2	5660	1743	69.2%
3	25022	2532	89.6%

- Oil formation volume factor increased significantly with CO₂ content. Once again a flattening trend, likely due to a liquid-liquid equilibrium region, was observed at high CO₂ mole fractions. Increases in swelling of up to 20% at high CO₂ saturation pressures, but values in the range of 5 - 7% would be more typical of values which could be reasonably obtained at saturation pressure values of less than 8 MPa.
- Gas solubility increased substantially as CO₂ saturation pressure was increased. Solubility decreased with API gravity, but gas solubilities of up to 74 m³/m³ (415 scf/bbl) were still obtained with even the heaviest oil (and values of almost 100 m³/m³ (561 scf/bbl) on the 15° API oil). Values typical of an 8 MPa field saturation pressure condition ranged in the 10 to 30 m³/m³ range indicating that a doubling of solution G.O.R. by CO₂ addition could be obtained even at relatively low operating pressures (< 8 MPa).
- CO₂ saturated oil densities were found to increase with increasing CO₂ content for the 15° and 12.4° API crude and to decrease for the low gravity 9.6° API crude. This inversion in density performance is likely related to the close similarity between oil and CO₂ densities and a crossover between pure oil and CO₂ component densities between the two higher API gravity systems and the low API gravity oil.

NUMERICAL CORRELATIONS

The data obtained in this study was utilized to provide global regression correlations with respect to:

- Viscosity (Table 8)
- Density (Table 9)
- Solubility (Table 10)
- Swelling (Table 11)

These predictive empirical formulations were constructed utilizing different five and six parameter functional formulations and utilized a non-linear Levenberg - Marquart optimization algorithm to determine the values of the regression constants which gave the closest possible match to the entire generated data set. The parameters were generated as functions of:

$\mu_o, \beta_o, G.O.R., \rho_o = F(\text{CO}_2 \text{ saturation pressure (MPa), oil stock tank API gravity and temperature (}^\circ\text{C)})$.

The correlations should be utilized only within the data limits specified in each table. Over this data range the correlations, in general, provide good approximations to the data set and are useful for interpolation to intermediate temperatures, CO₂ saturation pressures, or API gravities which were not evaluated as a portion of the study. Care should be exercised in utilizing the supplied correlations outside of the specified range of validity. It should also be remembered that these correlations are based on live (i.e., initially saturated with solution gas) oils and should not be considered accurate for dead or stock tank type crude oils.

COREFLOW TESTS

Procedures

The objectives of the coreflow tests were to determine if a significant amount of additional oil could be recovered at reservoir temperature through the use of CO₂. These tests were conducted utilizing actual samples of preserved state core material from the reservoirs from which each of the three oils originated. Two of the reservoirs were high permeability highly unconsolidated sands (oils #1 and #2) while Oil #3 was from a lower permeability lower quality sand interval.

The procedures utilized for these tests were as follows:

Oils #1 and #2 (15 and 12.4° API).

- Mount composite core approximately 50 - 60 cm in length (3.81 cm OD). Apply reservoir temperature and overburden pressure.
- Increase pore pressure to reservoir value (Oil #1 ≈ 4500 kPa, Oil #2 ≈ 3500 kPa) by dead oil injection.
- Displace dead oil with live reservoir crude oil until effluent G.O.R. matches initial live oil G.O.R.
- Conduct an unsteady state low rate waterflood at reservoir temperature to observe secondary recovery under straight waterflood conditions.
- Conduct a CO₂ water-alternating gas test with four (4) cycles of 0.10 PV CO₂ followed by a continuous waterflood to S_{br}. Note incremental oil recovery (if any) caused by the CO₂ injection.

Oil #3 (9.6° API)

1. Mount the composite core and saturate with dead and live oil (2600 kPa pore pressure) as for Oils #1 and #2. Due to the low permeability of the core and extremely high viscosity of the oil the oil the core had to be heated to approximately 80° C to mobilize the oil sufficiently to obtain injectivity.
2. Attempt a reservoir temperature waterflood and observe recovery.
3. Conduct an extended period (4 days) CO₂ soak at 3500 kPa pressure to attempt to mobilize oil.
4. Reflood with water at reservoir temperature and observe recovery.
5. Conduct a hot water/steamflood on the core at 260° C to compare effective recovery factor with CO₂.

EXPERIMENTAL EQUIPMENT - COREFLOOD TESTS

Figure 19 illustrates the experimental equipment used in the corefloods. The core material was mounted and encased, while frozen, in a thin teflon sleeve which was then heat shrunk onto the core. The encased core was sealed in a heavy lead sleeve in a Hassler-type core holder. The injection and production ends of the core were equipped with radial distribution plates to ensure evenly distributed fluid flow into and out of the core, and to eliminate areas of localized high velocity.

Overburden pressure was applied to the core by hydraulically pressurizing the annular space in the holder which applied a bi-axial stress to the core material.

Pressure differential across the core, which was measured to facilitate permeability calculations, was measured using two Validyne Model DP15 pressure transducers. The transducers were connected in a manifold arrangement having ranges of 0-350 kPa (0-50 psig) and 0-3500 kPa (0-500 psig) respectively. If the pressure differential across the core exceeded the pressure rating of the lower range transducer, it was isolated. The transducer outputted directly to a multi-channel Validyne terminal which provided an instantaneous reading of the pressure differential across the core. The transducer also outputted to a Hewlett-Packard multi-channel strip chart recorder which provided a continuous profile of the pressure differential across the core. Each of the transducers was accurate to 0.01% of the full scale value.

Backpressure, when required, was maintained through the use of a regulating backpressure valve. Fluids were injected using positive displacement Ruska pumps capable of injecting at rates from 1 cm³/hr to 240 cm³/hr and at pressures of up to 69 MPa with an accuracy of 0.01 cm³.

Samples were collected in a rotating fractionator apparatus and then subjected to high-speed centrifugation to determine produced oil and water volumes. If stable

emulsions were present, toluene was used to break the emulsion and was vacuum distilled from the oil. An atmospheric separator was used to measure the produced gas volume, if required.

COREFLOOD TEST RESULTS

Tables 12 - 14 and Figures 20 - 22 summarize the results of the three coreflow tests. From examination of this data it can be concluded that:

1. For Oils #1 and #2 significant additional recovery could be attributed to the use of CO₂ in a tertiary WAG mode. An additional 8.9% of the oil in place was recovered with Oil #1, and almost 16% additional recovery was noted for Oil #2. The higher recovery factor for the heavier oil system is likely related to the much superior reservoir quality existing in the Oil #2 system (7722 mD permeability) in comparison to a much lower 918 mD permeability for the Oil #1 test. The higher reservoir quality likely contributes to greater sweep efficiency due to a larger pore size distribution and also likely much greater and easier contact of the oil in place by the injected CO₂.
2. For Oil #3, no water injectivity could initially be obtained at the reservoir temperature of 22° C due to a combination of low reservoir permeability and high reservoir temperature oil viscosity (a zero percent waterflood recovery factor). However, it is very interesting to note that after the CO₂ soak treatment at reservoir temperature that 11.2% of the oil in place was mobilized indicating a significant beneficial effect by the CO₂ contact.
3. The hot water and steamflood test resulted in substantial additional reduction of the residual oil saturation for the Oil #3 test. This would appear to indicate that, while CO₂ injection processes have application in increasing secondary and tertiary recovery factors, particularly in high quality reservoirs and for higher gravity crude oils, that thermal stimulation techniques still appear to have the greatest potential for obtaining low (i.e., <20%) residual oil saturations in low API gravity crude oils. Combinations of CO₂ and thermal stimulation (such as steam/CO₂ treatments or in-situ combustion processes) likely benefit substantially from the inclusion of the CO₂, but the actual degree of enhancement was not specifically measured as a portion of this study.

CONCLUSIONS

1. The use of CO₂ was found to substantially reduce viscosity and increase swelling and gas solubility in three different solution gas saturated heavy oil systems ranging from 9.6 to 15° API. Substantial reductions in viscosity were noted at CO₂ saturation pressures of less than 8 MPa and significant reductions (in excess of 95%) at CO₂ saturation pressures of 19 MPa. No evidence of asphaltene precipitation problems associated with contact by the CO₂ were observed for any of the oils.

2. General correlations were developed as a result of this work to predict the density, viscosity, swelling and solubility of live oil-CO₂ systems as a function of API gravity, CO₂ saturation pressure and temperature.
3. Coreflow studies indicated that significant (9 - 16%) oil could be recovered from heavy oil reservoirs through the use of immiscible CO₂ in a tertiary mode. The use of CO₂ however, still does not appear to yield residual oil saturations as low as obtained from conventional high temperature steamflood operations. Carbon dioxide may be a viable consideration in many deeper heavy oil reservoirs where heat losses to the overburden may render steamflooding uneconomical and the greater natural pressure in some of these types of reservoirs will enhance the solubility and beneficial effects of CO₂ stimulation.

TABLE 1
Properties and Composition of Tested Oils

Component	Oil #1	Oil #2	Oil #3
N ₂	0.0021	0.0000	0.0000
CO ₂	0.0006	0.0000	0.0000
H ₂ S	0.0004	0.0000	0.0000
C ₁	0.1824	0.1486	0.1060
C ₂	0.0096	0.0000	0.0000
C ₃	0.0016	0.0000	0.0000
i-C ₄	0.0014	0.0000	0.0000
n-C ₄	0.0006	0.0000	0.0000
i-C ₅	0.0032	0.0000	0.0000
n-C ₅	0.0003	0.0000	0.0000
C ₆	0.7982	0.8514	0.8940
Density (kg/m ³)@ 15° C	965.9	983.3	1002.8
°API	15.0	12.4	9.6
Reservoir Temperature (°C)	27.0	20.0	22.0
Saturation Pressure (kPa.s)	4482	3495	2503
Initial GOR (m ³ /m ³)	13.02	9.80	6.30
Initial Live Oil Density (kg/m ³)	947.1	966.0	999.0
% Asphaltene (mass)	10.0%	15.0%	17.0%

TABLE 2
Saturation Pressure Variation With Temperature
And CO₂ Concentration, Oil #1 (15° API)

27° C		100° C		175° C	
Mole Fraction CO ₂	Saturation Pressure (kPag)	Mole Fraction CO ₂	Saturation Pressure (kPag)	Mole Fraction CO ₂	Saturation Pressure (kPag)
0.0000	4482	0.0000	6135	0.0000	7239
0.0832	5860	0.1124	9860	0.1794	8963
0.2505	8790	0.2947	12240	0.2656	12928
0.3260	10860	0.3869	16200	0.6091	15926
0.3883	13513	0.4142	18270	0.6896	18271
0.7270	16547				

TABLE 3
Saturation Pressure Variation With Temperature
And CO₂ Concentration, Oil #2 (12.4° API)

20° C		100° C		175° C	
Mole Fraction CO ₂	Saturation Pressure (kPag)	Mole Fraction CO ₂	Saturation Pressure (kPag)	Mole Fraction CO ₂	Saturation Pressure (kPag)
0.0000	3495	0.0000	6757	0.0000	7239
0.2528	7930	0.2371	9791	0.2457	10894
0.3401	9135	0.3830	12342	0.2816	13445
0.5489	12065	0.4554	16444	0.3224	14824
0.6642	15170	0.4822	19098	0.3904	19030

TABLE 4
Saturation Pressure Variation With Temperature
And CO₂ Concentration, Oil #3 (9.6° API)

22° C		100° C		175° C	
Mole Fraction CO ₂	Saturation Pressure (kPag)	Mole Fraction CO ₂	Saturation Pressure (kPag)	Mole Fraction CO ₂	Saturation Pressure (kPag)
0.0000	2503	0.0000	3613	0.0000	4482
0.3011	6274	0.1428	5522	0.0505	5964
0.3869	9584	0.4220	10611	0.2190	9032
0.4847	11928	0.4729	11872	0.4287	13031
0.5390	12686	0.5929	15671	0.8323	17065
0.6781	13066				

TABLE 5
Oil #1, 15° API, Measured Physical Properties
As a Function of CO₂ Concentration

Temperature- 27°C					Temperature- 100°C					Temperature- 175°C				
CO ₂ Saturation Pressure kPag	Viscosity (mPa.s)	Swelling Factor	Gas-Oil Ratio (m ³ /m ³)	Density (kg/m ³)	CO ₂ Saturation Pressure kPag	Viscosity (mPa.s)	Swelling Factor	Gas-Oil Ratio (m ³ /m ³)	Density (kg/m ³)	CO ₂ Saturation Pressure kPag	Viscosity (mPa.s)	Swelling Factor	Gas-Oil Ratio (m ³ /m ³)	Density (kg/m ³)
4482	953	1.000	13.0	947.1	6135	27.2	1.000	13.0	922.0	7239	7.0	1.000	13.0	860.1
5860	834	1.020	17.8	933.6	9860	12.6	1.035	23.2	924.0	8963	5.2	1.015	21.0	862.0
8790	171	1.062	28.8	949.6	12240	11.1	1.071	33.5	924.5	12928	3.0	1.060	36.4	863.0
10860	75	1.093	68.6	957.6	16200	8.0	1.150	65.9	925.0	15926	2.5	1.120	48.0	866.0
13513	30	1.124	84.6	965.9	18270	5.6	1.222	86.8	926.0	18271	2.4	1.199	57.3	869.0
16547	22	1.201	98.0	970.0										

TABLE 6
Oil #2, 12.4° API, Measured Physical Properties
As a Function of CO₂ Concentration

Temperature- 20°C					Temperature- 100°C					Temperature- 175°C				
CO ₂ Saturation Pressure kPag	Viscosity (mPa.s)	Swelling Factor	Gas-Oil Ratio (m ³ /m ³)	Density (kg/m ³)	CO ₂ Saturation Pressure kPag	Viscosity (mPa.s)	Swelling Factor	Gas-Oil Ratio (m ³ /m ³)	Density (kg/m ³)	CO ₂ Saturation Pressure kPag	Viscosity (mPa.s)	Swelling Factor	Gas-Oil Ratio (m ³ /m ³)	Density (kg/m ³)
3495	5660	1.000	9.8	966.0	6757	36.0	1.000	9.8	955.0	7239	10.0	1.000	9.8	933.0
7930	1743	1.069	35.5	967.0	9791	12.5	1.030	17.0	963.0	10894	6.3	1.025	13.0	943.0
9135	1042	1.095	65.2	972.0	12342	6.6	1.061	25.5	966.0	13445	3.2	1.048	16.5	953.0
12065	464	1.124	77.3	976.0	16444	5.9	1.103	50.9	968.0	14824	3.2	1.089	26.6	960.0
15170	196	1.155	88.0	980.0	19098	5.5	1.125	83.0	973.0	19030	3.4	1.113	46.4	965.0

TABLE 8
Global Viscosity Correlation

$\log_{10}(\log_{10}(\mu_o)) = A1 + A2 * (T + 273.15) + A3 * P + A4 * \frac{P}{(T + 273.15)} + A5 * \frac{T^2}{P} + A6 * API$	
where: μ_o	= live oil viscosity (cP or mPa.s) at pressure and temperature
P	= CO ₂ saturation pressure (MPa gauge)
T	= temperature (°C)
°API	= stock tank oil API gravity at 15.56°C and 101.325 kPa (°API = 141.5/P _o - 131.5)
Regression Constants:	A1 = 1.93823875 A2 = -0.00380987 A3 = -0.03229645 A4 = 4.32733524 A5 = 0.00002880 A6 = -0.01923601
Range of Validity:	9.5 < API < 16 20 < T < 175°C 4.0 < P < 20.0 MPA
Error in means of predicted and experimental data - 509 mPa.s	
Average least square error (standard deviation) over entire data range = 2563 mPa.s	

TABLE 9
Global Density Correlation

$\rho = A1 + A2 * P + A3 * T + A4 * T^2 + A5 * \text{°API}$	
where: ρ	= density of oil at pressure and temperature (g/cm ³)
P	= CO ₂ saturation pressure (MPa gauge)
T	= absolute temperature (K) = (°C + 273.15)
°API	= oil stock tank oil API gravity at 15.56°C, 101.325 kPa (°API = 141.5/P _o - 131.5)
Regression Constants:	A1 = 0.98384779 A2 = 0.00058215 A3 = 0.00072928 A4 = -0.00000151 A5 = -0.00812997
Range of Validity:	12 < API < 16 20 < T < 175°C 3.0 < P < 20.0 MPA
Error in means of predicted and experimental and predicted data = 0.00031 g/cm ³	
Average least square error (standard deviation) over entire data range = 0.0189 g/cm ³	

TABLE 10
Solubility Expression

$\log_{10} (RSI) = A1 * \left(\frac{P^2}{T} \right) + A2 * P + A3 * \left(\frac{P}{T} \right) + A4 * \left(\frac{P^2}{T^2} \right) + A5 * T^2 + A6 * \text{°API}$	
where: RSI	= solution gas-oil ratio (m ³ /m ³ or ft ³ /ft ³)
P	= CO ₂ saturation pressure (MPa gauge)
T	= absolute temperature (K) = (°C + 273.15)
°API	= oil stock tank oil API gravity at 15.56°C, 101.325 kPa (°API = 141.5/ρ _o - 131.5)
Regression Constants:	A1 = 0.080135200 A2 = -0.0252479875 A3 = 43.974164963 A4 = -177.409627914 A5 = -0.000000008657 A6 = 0.0355611741
Range of Validity:	9.5 < API < 16 20 < T < 175°C 4.0 < P < 20.0 MPA
Error in means of experimental and predicted data	m ³ /m ³ = 6.56
Average least square error (standard deviation) over entire data	range = 12.3 m ³ /m ³

TABLE 11
Solubility Expression

$\log_{10} (Swell) = A1 + A2 * P + A3 * T + A4 * T^2 + A5 * \text{°API}$	
where: Swell	= Swelling (CO ₂ saturated oil volume/live oil volume at pressure and temperature)
P	= CO ₂ saturation pressure (MPa gauge)
T	= absolute temperature (K) = (°C + 273.15)
°API	= oil stock tank oil API gravity at 15.56°C, 101.325 kPa (°API = 141.5/ρ _o - 131.5)
Regression Constants:	A1 = 0.16882708 A2 = 0.00487583 A3 = -0.00099704 A4 = 0.00000116 A5 = 0.00085532
Range of Validity:	9.5 < °API < 15.5 20 < T < 70°C 5.0 < P < 16 MPa 71 < T < 130°C 6.0 < P < 17 MPa 131 < T < 175°C 7.0 < P < 18 MPa
Error in means of experimental and predicted data	vol/vol = 0.00034
Average least square error (standard deviation) over entire data	range = 0.0255 vol/vol

TABLE 12
Coreflow Test Conducted
Utilizing Oil #1 (15° API)

Test Phase	So	Sw	% Recovery (cuml)	Effective Permeability		Relative Permeability
				$(\mu m)^2 \times 10^{-3}$	(mD)	
Initial Live Oil @ 20° C	0.637	0.363	--	724.0	734.0	0.800
Waterflood @ 27° C	0.471	0.529	26.0	13.4	13.6	0.015
Water-CO ₂ WAG @ 27° C	0.414	0.586	34.9	38.2	38.7	0.042
Core Parameters - Absolute permeability $905 \times 10^{-3} (\mu m)^2$ [918 mD] - Porosity - 31.8%						

TABLE 13
Coreflow Test Conducted
Utilizing Oil #2 (12.4° API)

Test Phase	So	Sw	% Recovery (cuml)	Effective Permeability		Relative Permeability
				$(\mu m)^2 \times 10^{-3}$	(mD)	
Initial Live Oil @ 20° C	0.886	0.114	--	6826	6916	0.896
Waterflood @ 27° C	0.616	0.384	30.5	24.36	24.68	0.0032
Water-CO ₂ WAG @ 27° C	0.477	0.557	46.2	77.2	78.2	0.010
Core Parameters - Absolute permeability $905 \times 10^{-3} (\mu m)^2$ [918 mD] - Porosity - 31.8%						

TABLE 14
Coreflow Test Conducted
Utilizing Oil #3 (9.6 °API)

Test Phase	So	Sw	% Recovery (cuml)	Effective Permeability		Relative Permeability
				$(\mu m)_3^2 \times 10^6$	(mD)	
Initial Live Oil @ 20°C	0.607	0.393	--	Immobile	Immobile	N/A
Waterflood @ 27°C	0.607	0.393	--	Immobile	Immobile	N/A
Water-CO ₂ @ 27°C	0.539	0.461	11.2	0.514	0.521	N/A
Hot Water/Steam @ 260°C	0.132	0.868	78.2	0.674	0.683	N/A
Core Parameters - Absolute permeability - not available - Porosity - 30.7%						

Figure 1
Typical Low Temperature
CO₂-Oil Phase Behaviour

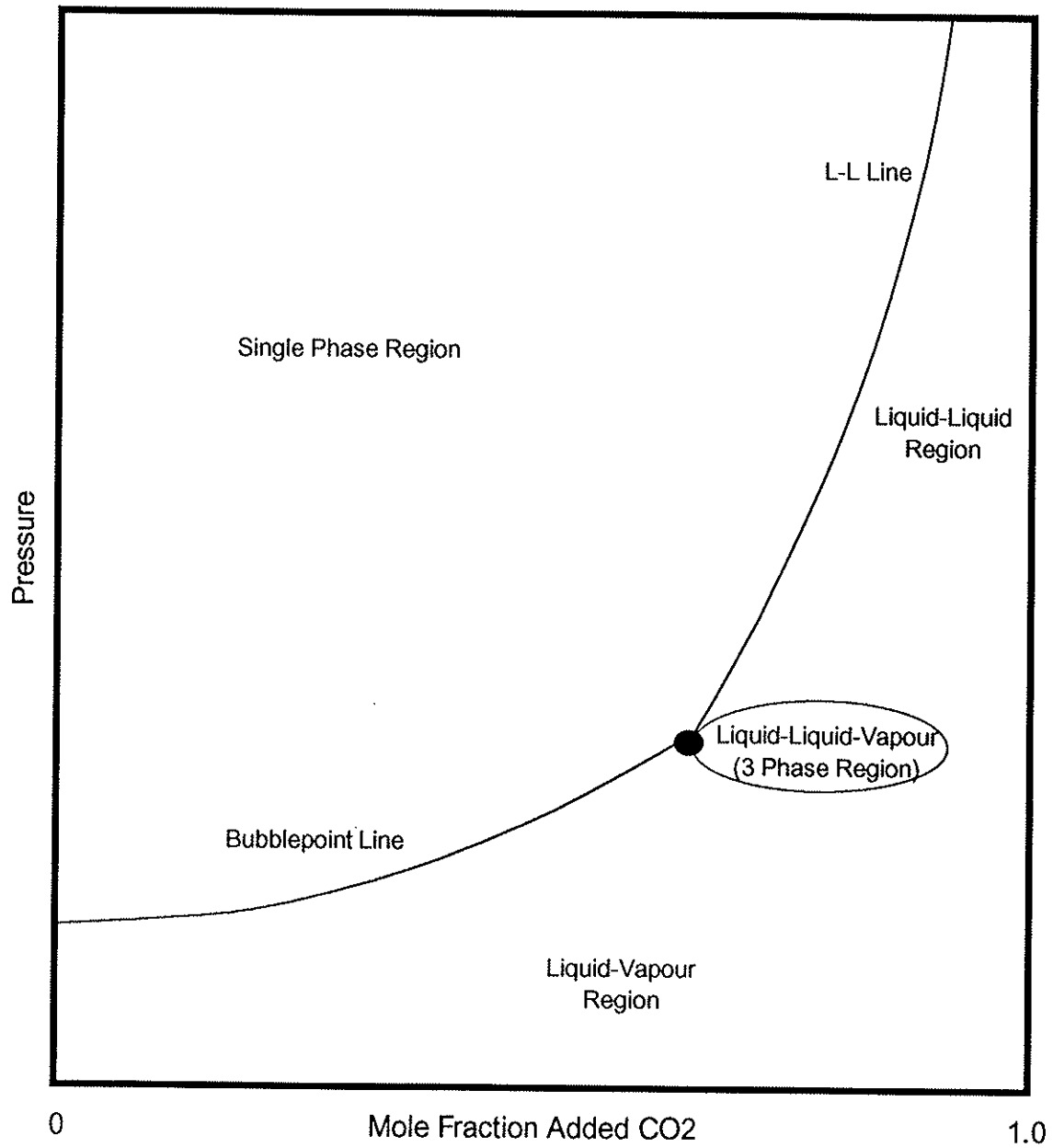


FIGURE 2
Typical Pressure - Temperature
Phase Behaviour Response

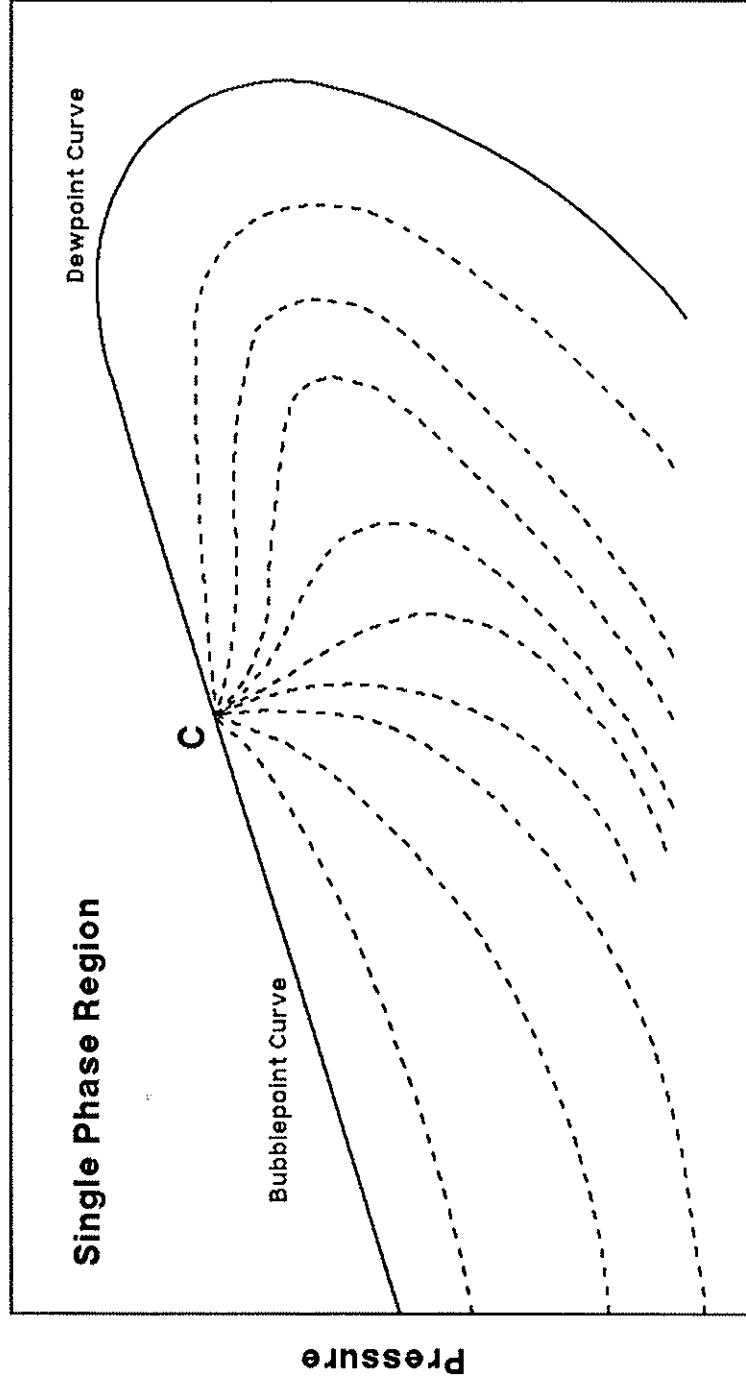


FIGURE 3
HEAVY OIL PVT APPARATUS

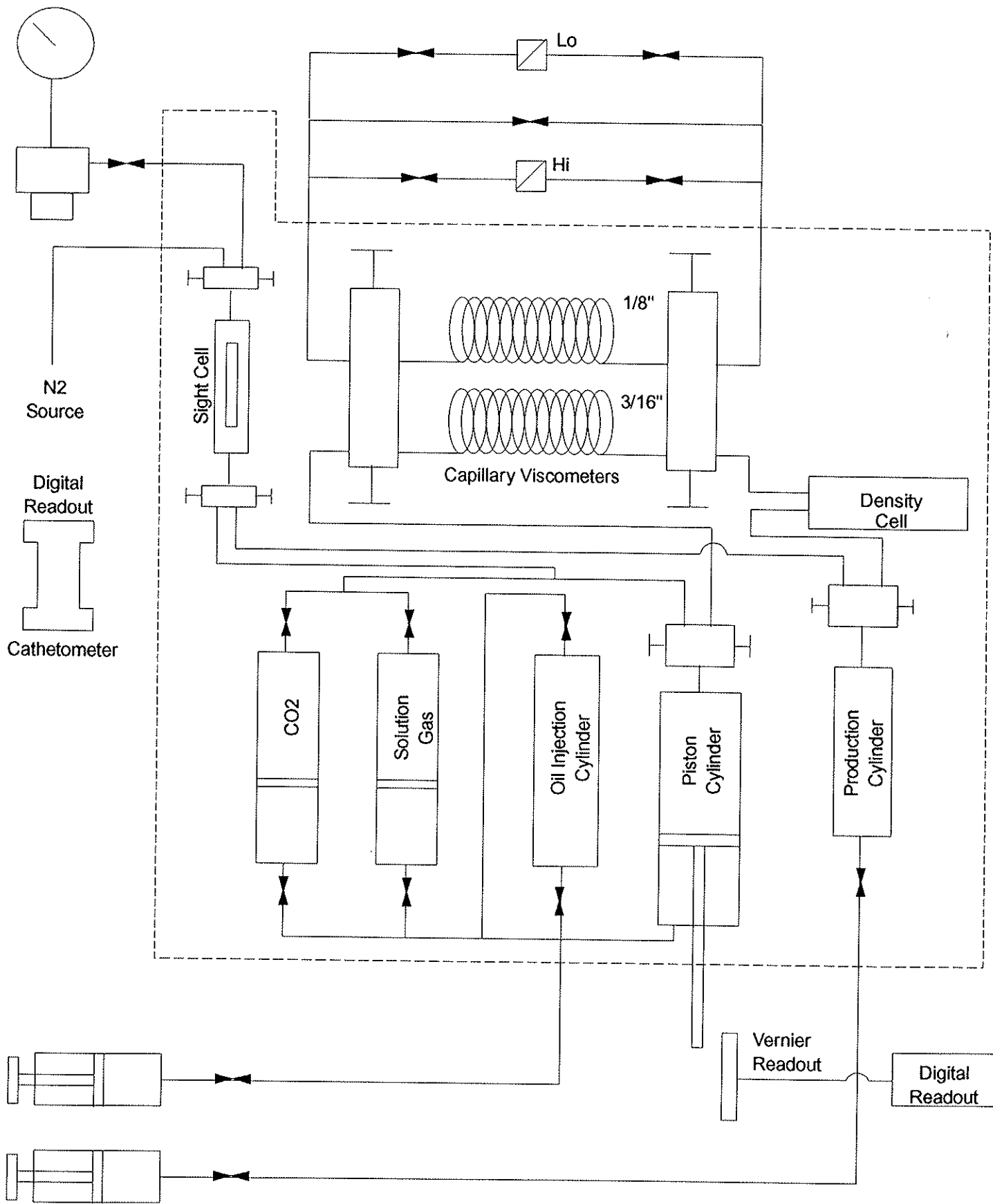


FIGURE 4
Psat VARIATION WITH TEMPERATURE & CO2 CONCENTRATION
OIL #1 (15°API)
SATURATION PRESSURE vs MOLE FRACTION CO2

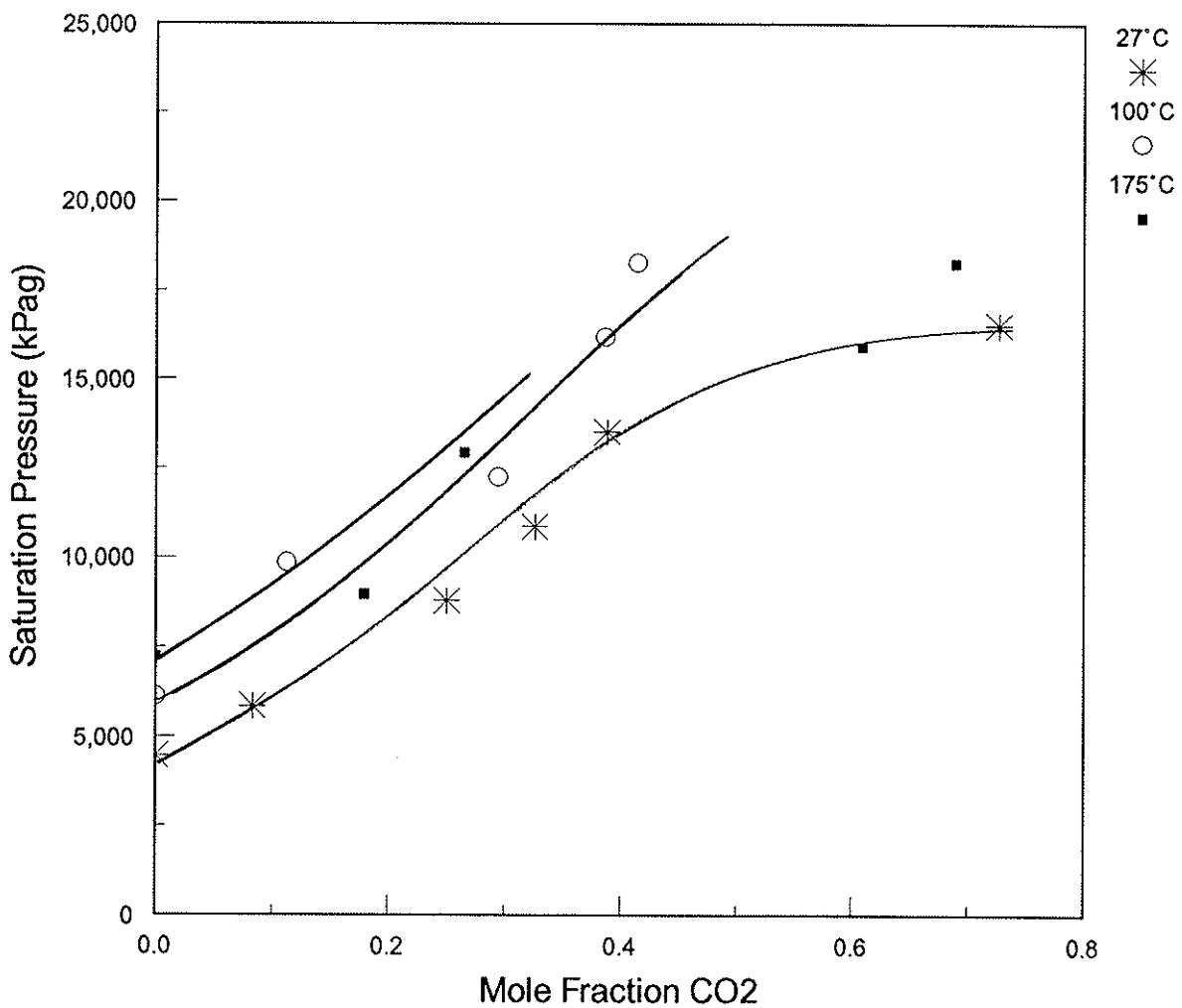


FIGURE 5
Psat VARIATION WITH TEMPERATURE & CO2 CONCENTRATION
OIL #2 (12.4° API)
SATURATION PRESSURE vs MOLE FRACTION CO2

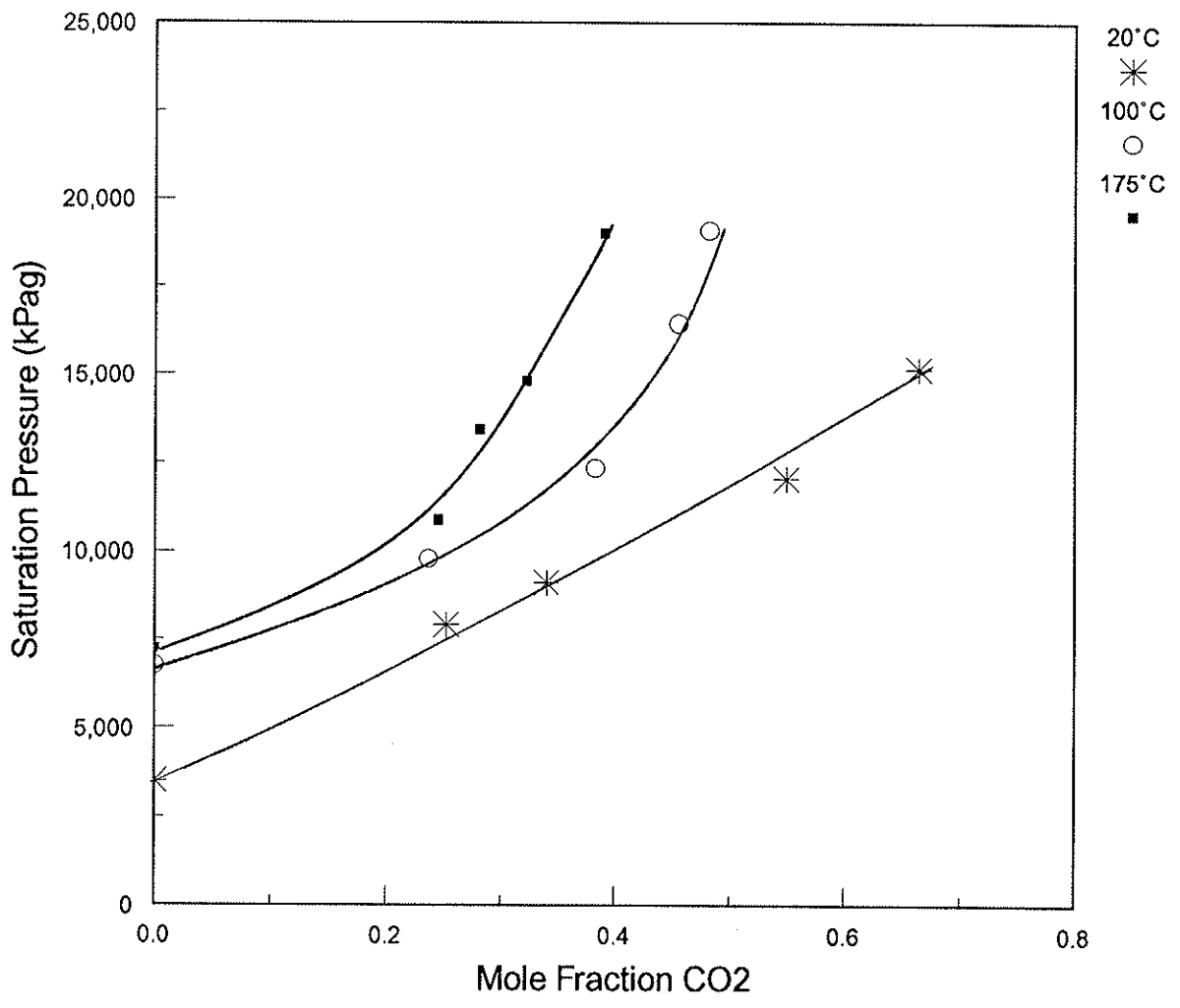


FIGURE 6
Psat VARIATION WITH TEMPERATURE & CO2 CONCENTRATION
OIL #3 (9.6° API)
SATURATION PRESSURE vs MOLE FRACTION CO2

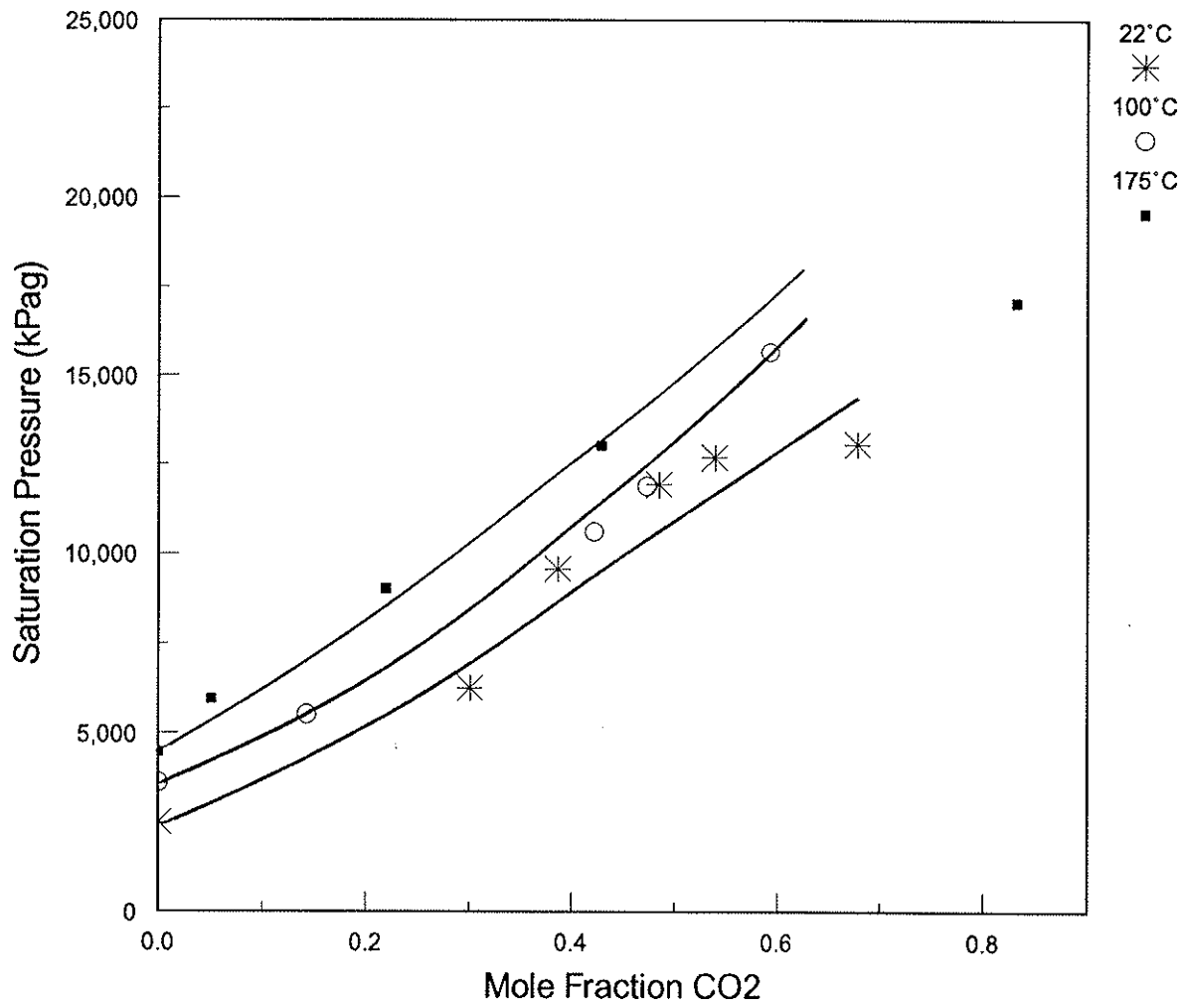


FIGURE 7
MEASURED PHYSICAL PROPERTIES AS A FUNCTION OF CO2 CONCENTRATION
OIL #1 (15° API)
VISCOSITY vs SATURATION PRESSURE

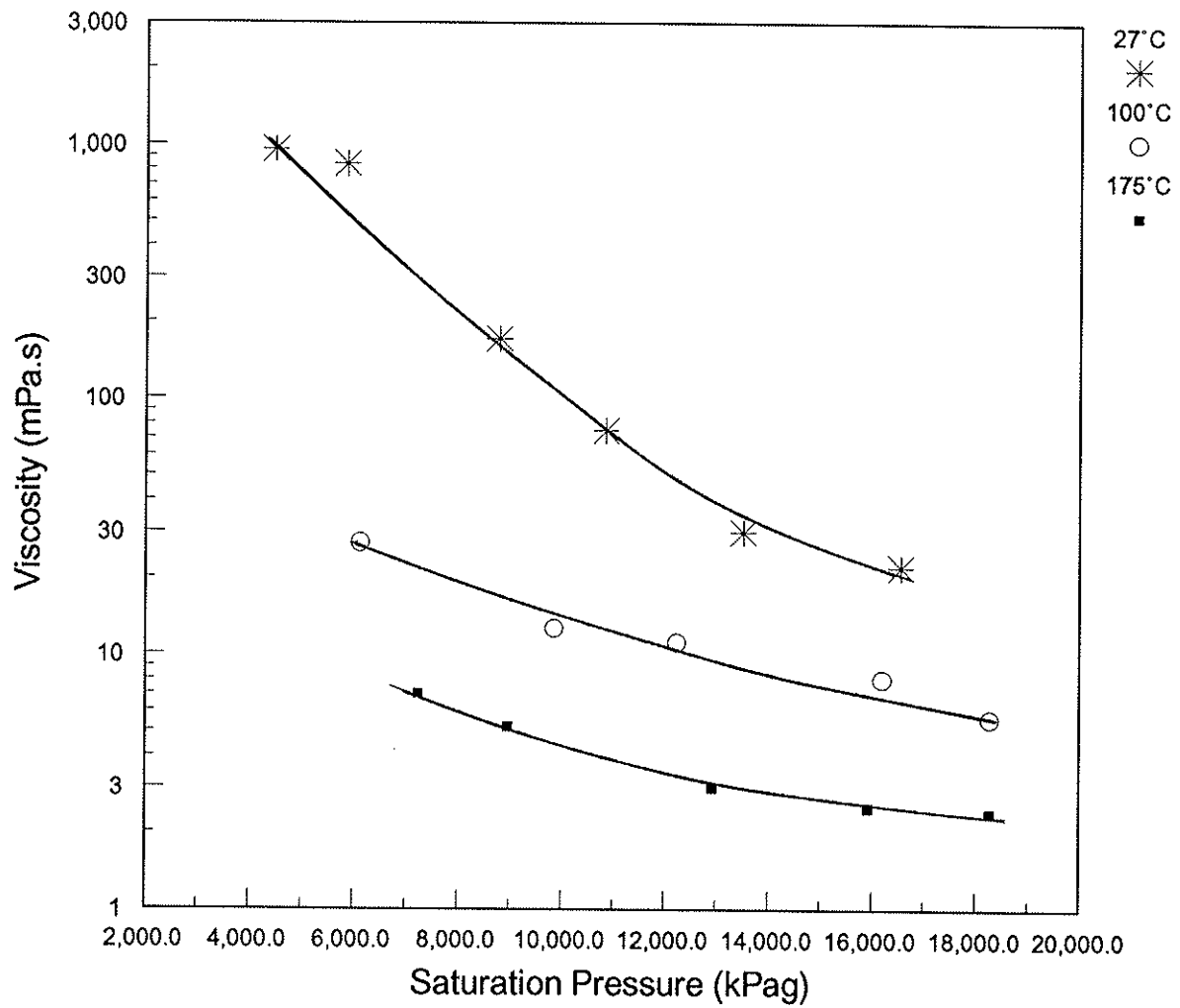


FIGURE 8
MEASURED PHYSICAL PROPERTIES AS A FUNCTION OF CO2 CONCENTRATION
OIL #1 (15° API)
SWELLING FACTOR vs SATURATION PRESSURE

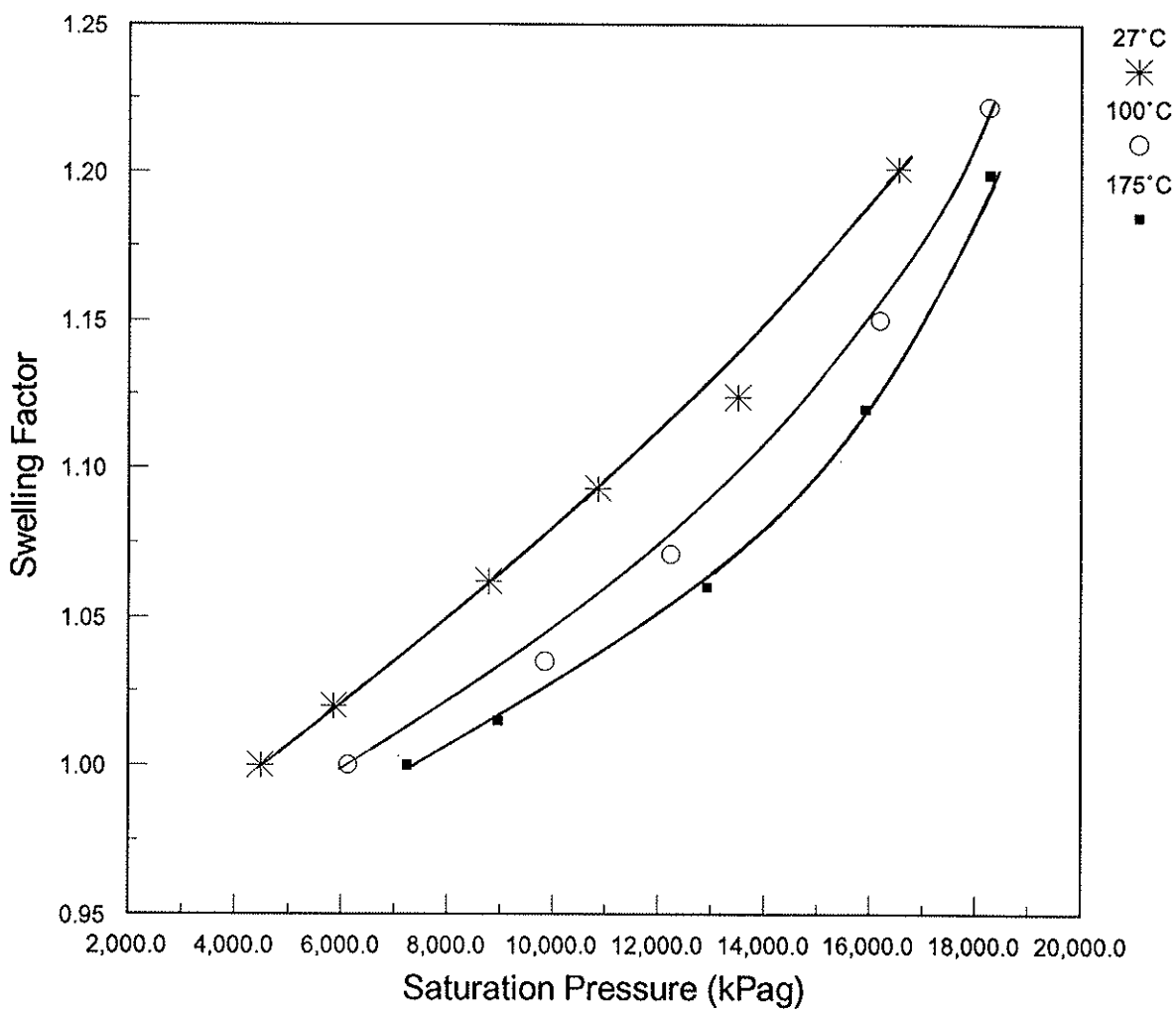


FIGURE 9
MEASURED PHYSICAL PROPERTIES AS A FUNCTION OF CO2 CONCENTRATION
OIL #1 (15° API)
GOR vs SATURATION PRESSURE

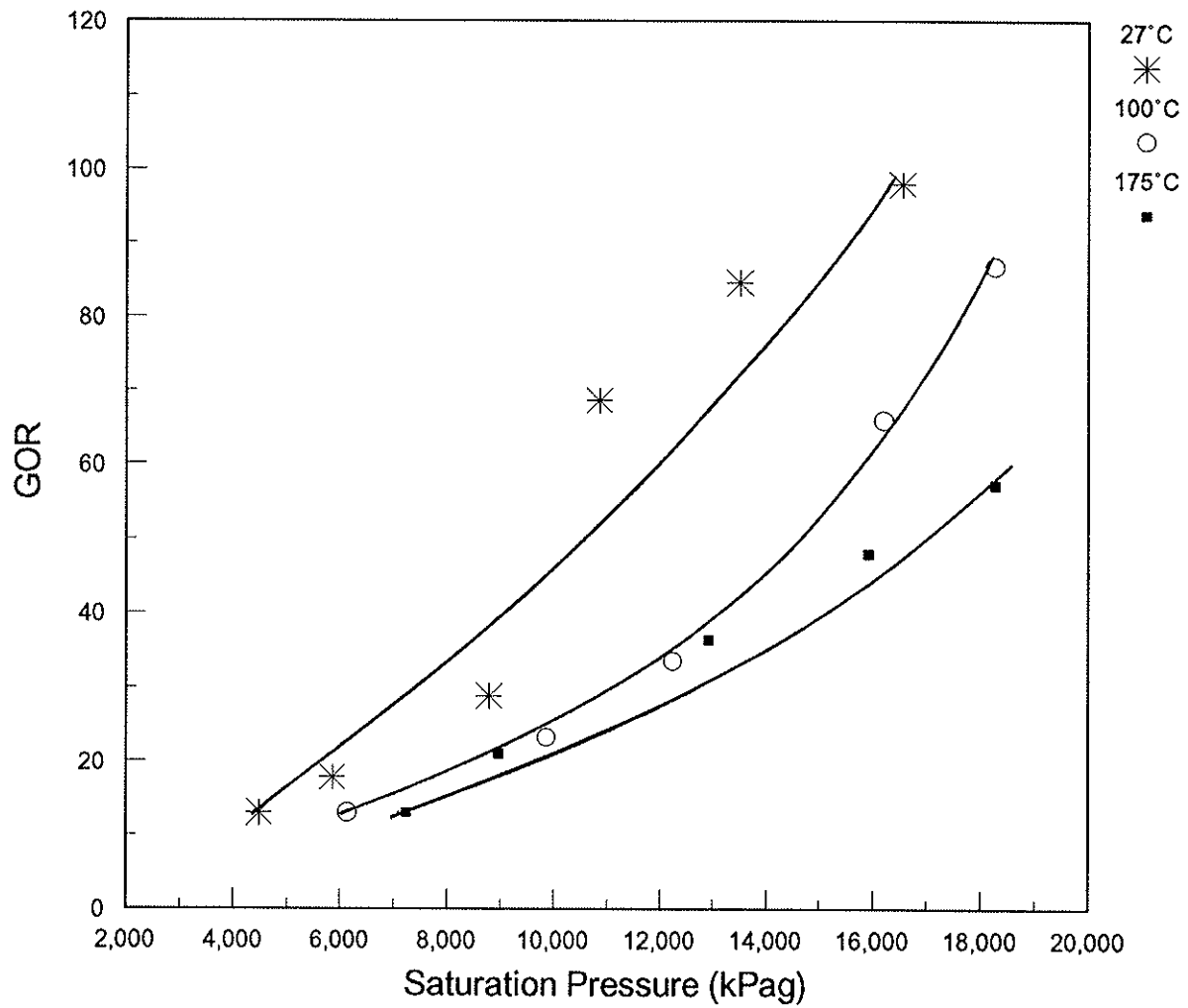


FIGURE 10
MEASURED PHYSICAL PROPERTIES AS A FUNCTION OF CO2 CONCENTRATION
OIL #1 (15°API)
DENSITY vs SATURATION PRESSURE

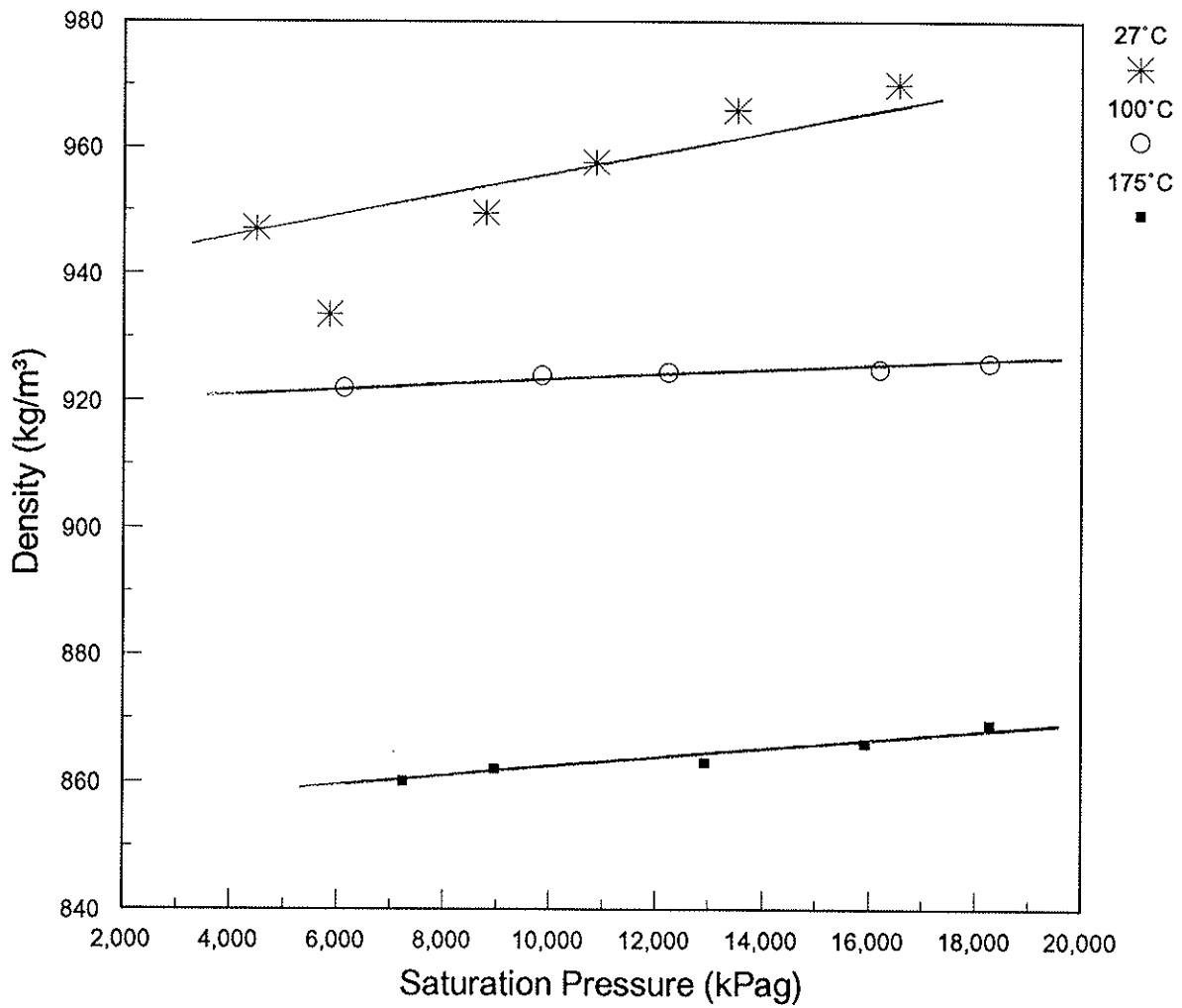


FIGURE 11
MEASURED PHYSICAL PROPERTIES AS A FUNCTION OF CO2 CONCENTRATION
OIL #2 (12.4°API)
VISCOSITY vs SATURATION PRESSURE

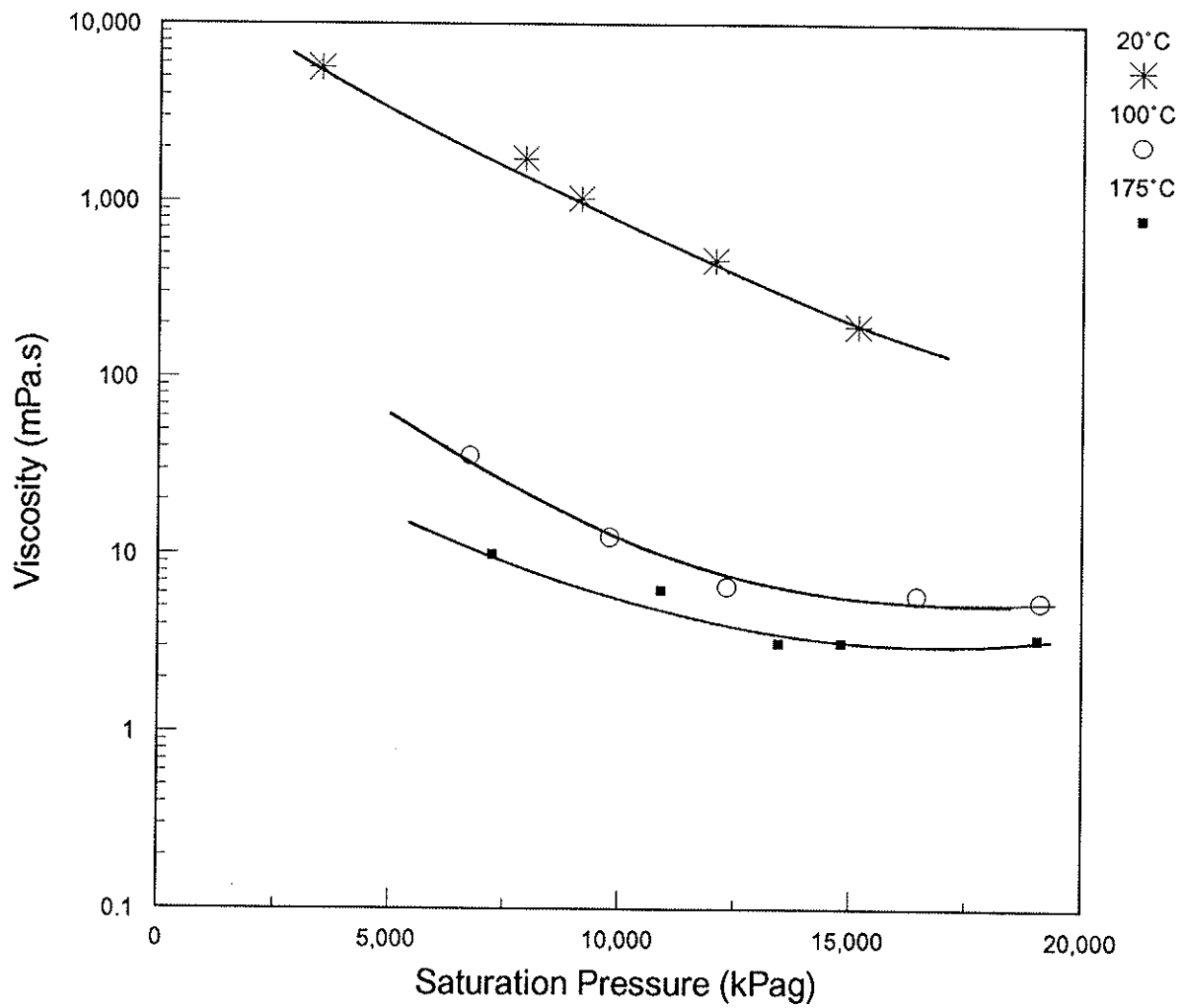


FIGURE 12
MEASURED PHYSICAL PROPERTIES AS A FUNCTION OF CO2 CONCENTRATION
OIL #2 (12.4°API)
SWELLING FACTOR vs SATURATION PRESSURE

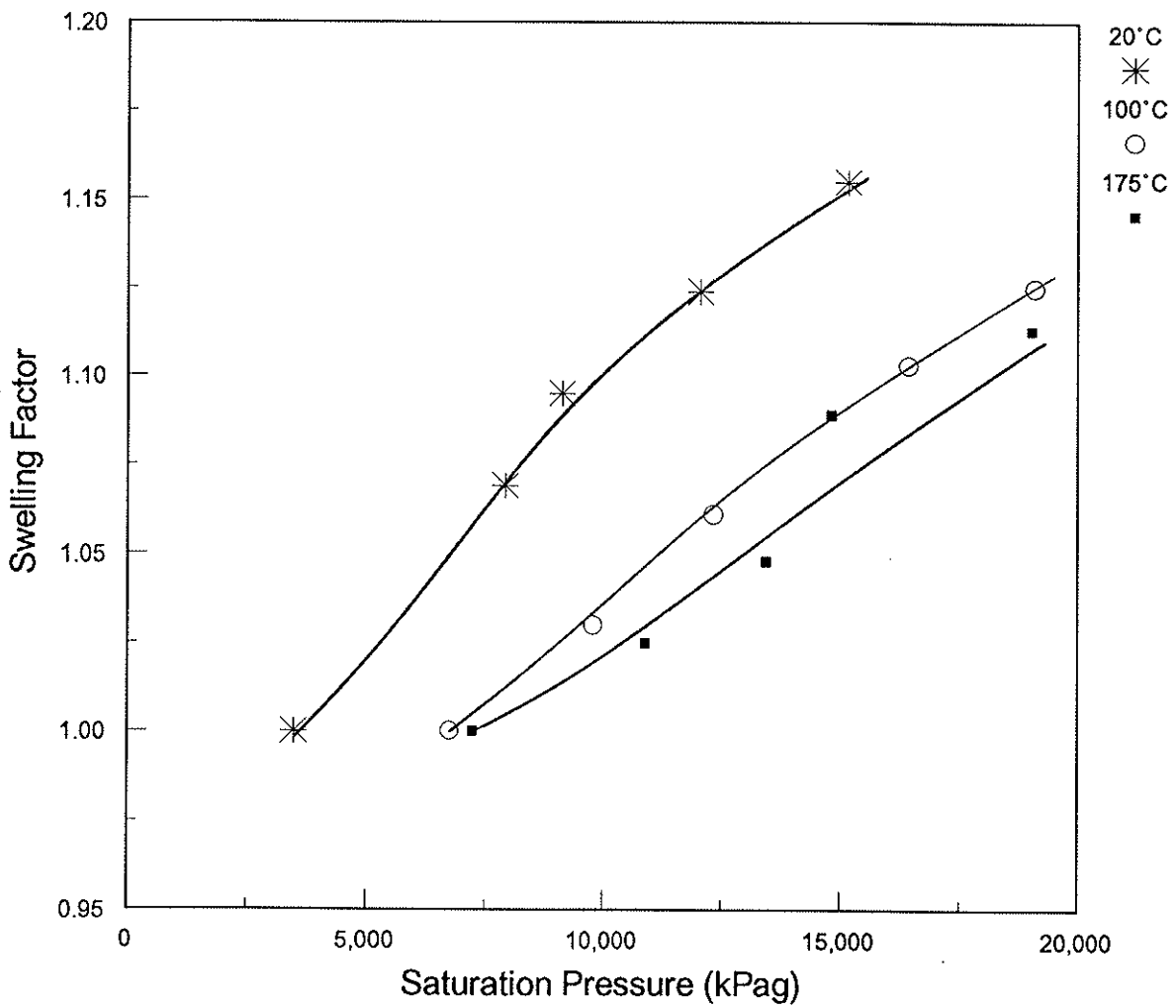


FIGURE 13
MEASURED PHYSICAL PROPERTIES AS A FUNCTION OF CO2 CONCENTRATION
OIL #2 (12.4° API)
GOR vs SATURATION PRESSURE

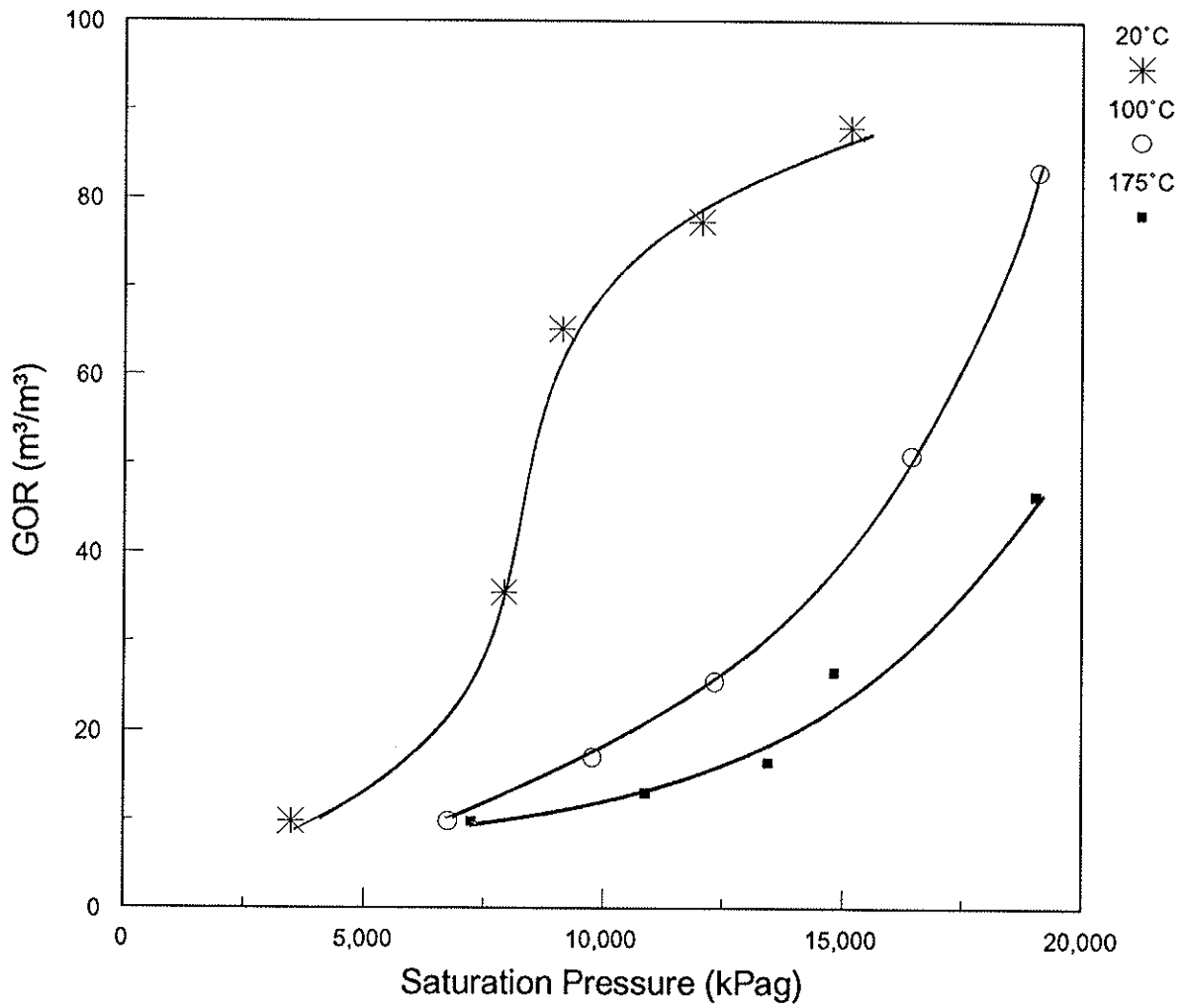


FIGURE 14
MEASURED PHYSICAL PROPERTIES AS A FUNCTION OF CO2 CONCENTRATION
OIL #2 (12.4° API)
DENSITY vs SATURATION PRESSURE

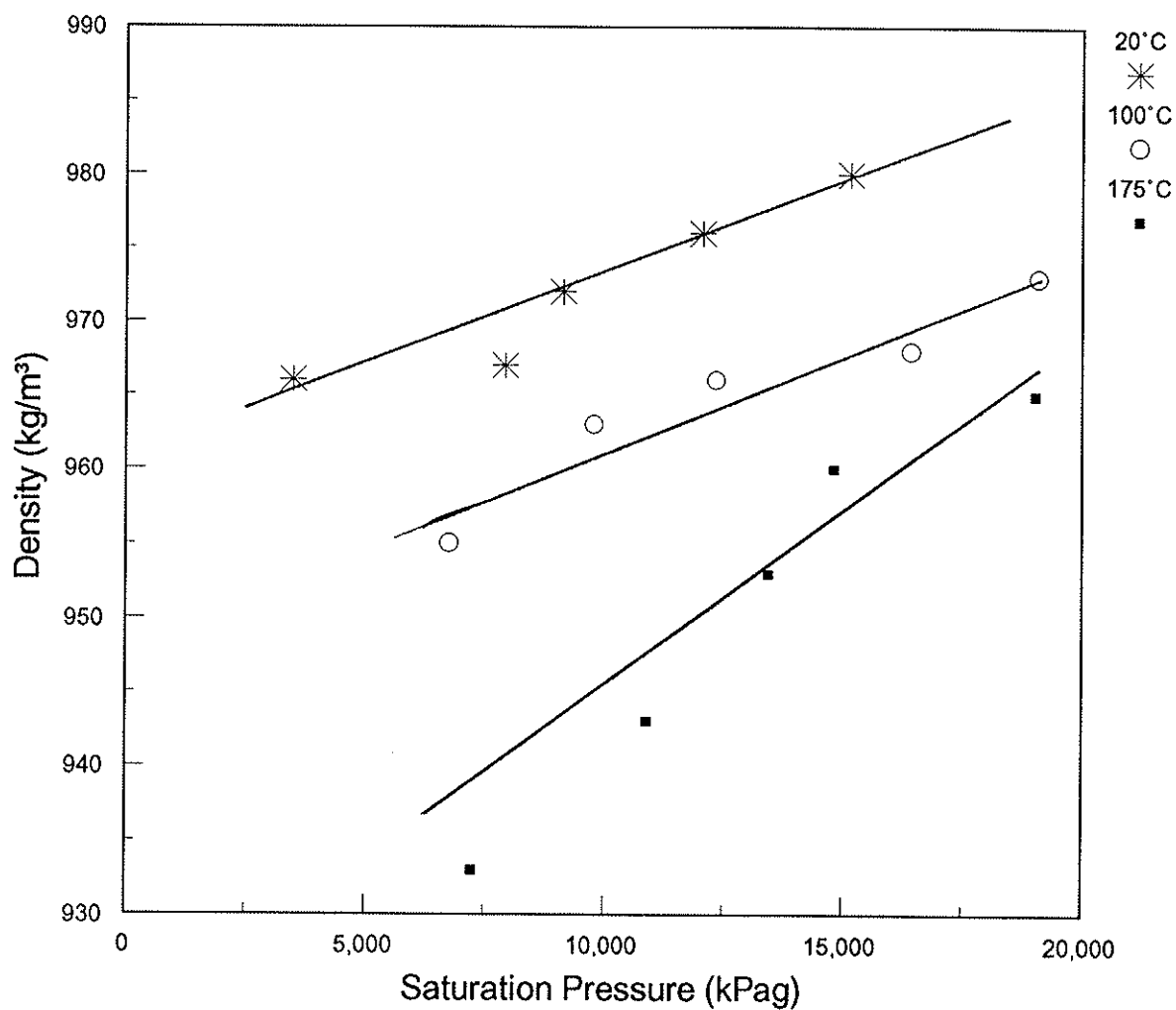


FIGURE 15
MEASURED PHYSICAL PROPERTIES AS A FUNCTION OF CO2 CONCENTRATION
OIL #3 (9.6° API)
VISCOSITY vs SATURATION PRESSURE

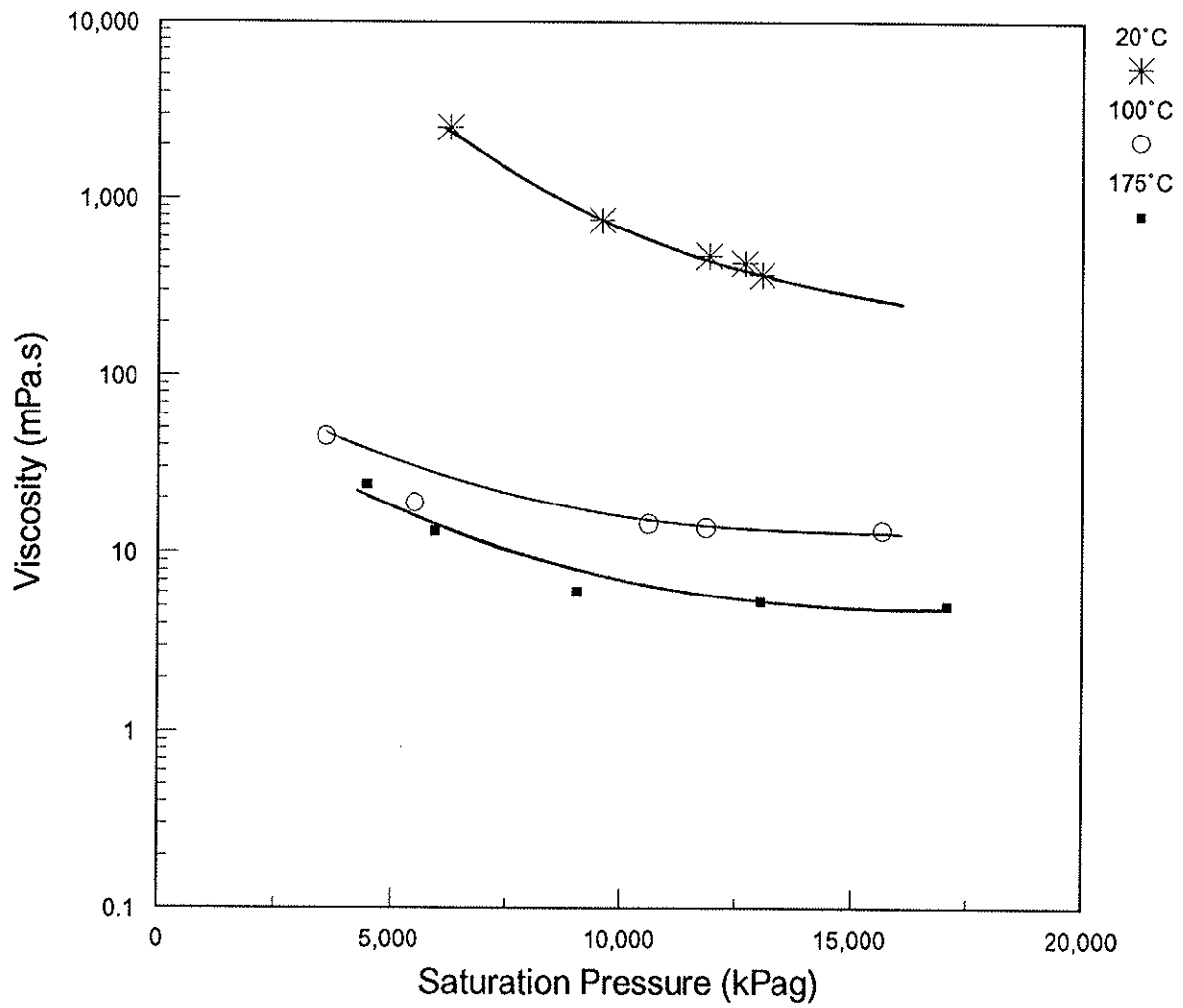


FIGURE 16
MEASURED PHYSICAL PROPERTIES AS A FUNCTION OF CO2 CONCENTRATION
OIL #3 (9.6° API)
SWELLING FACTOR vs SATURATION PRESSURE

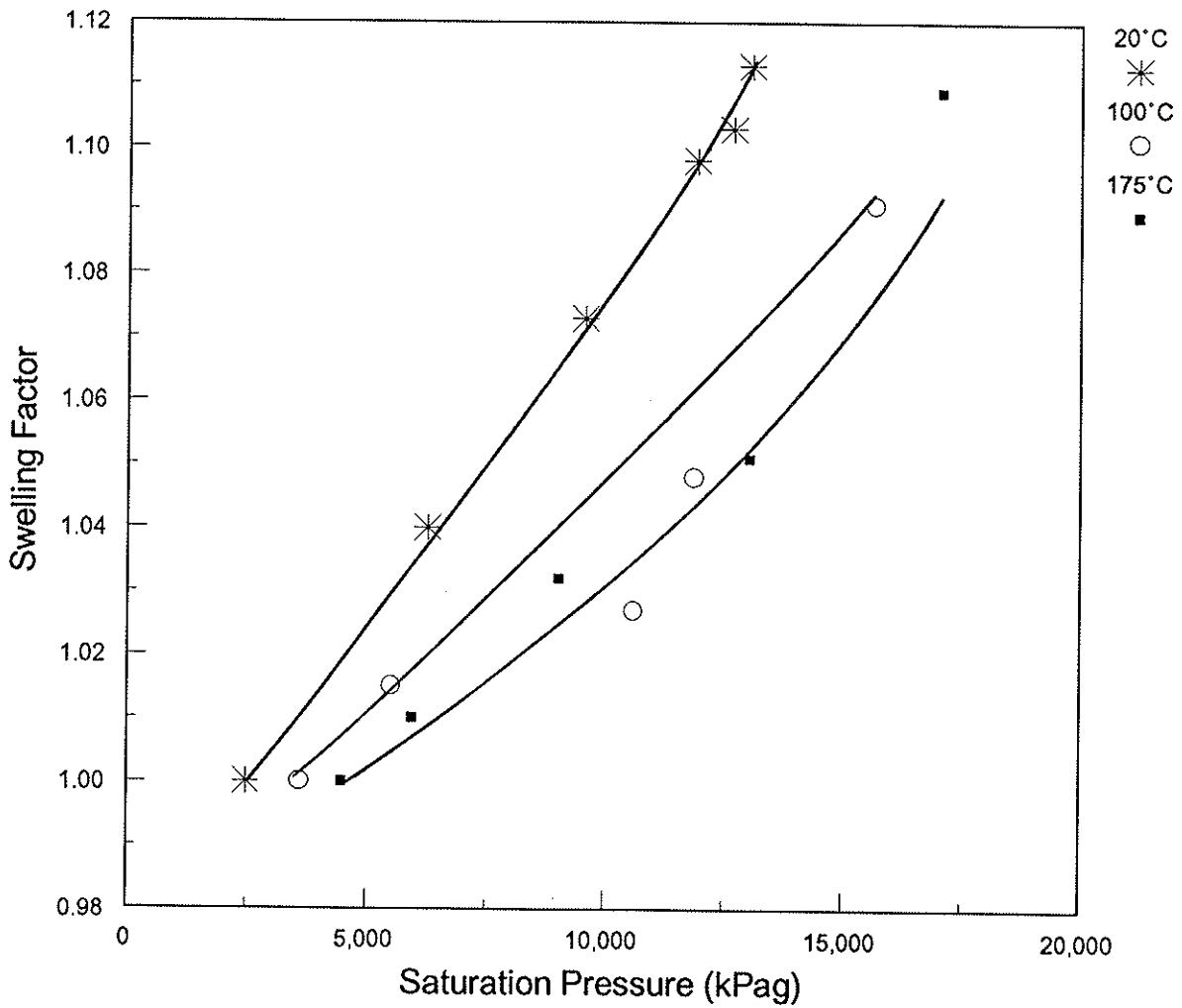


FIGURE 17
MEASURED PHYSICAL PROPERTIES AS A FUNCTION OF CO2 CONCENTRATION
OIL #3 (9.6° API)
GOR vs SATURATION PRESSURE

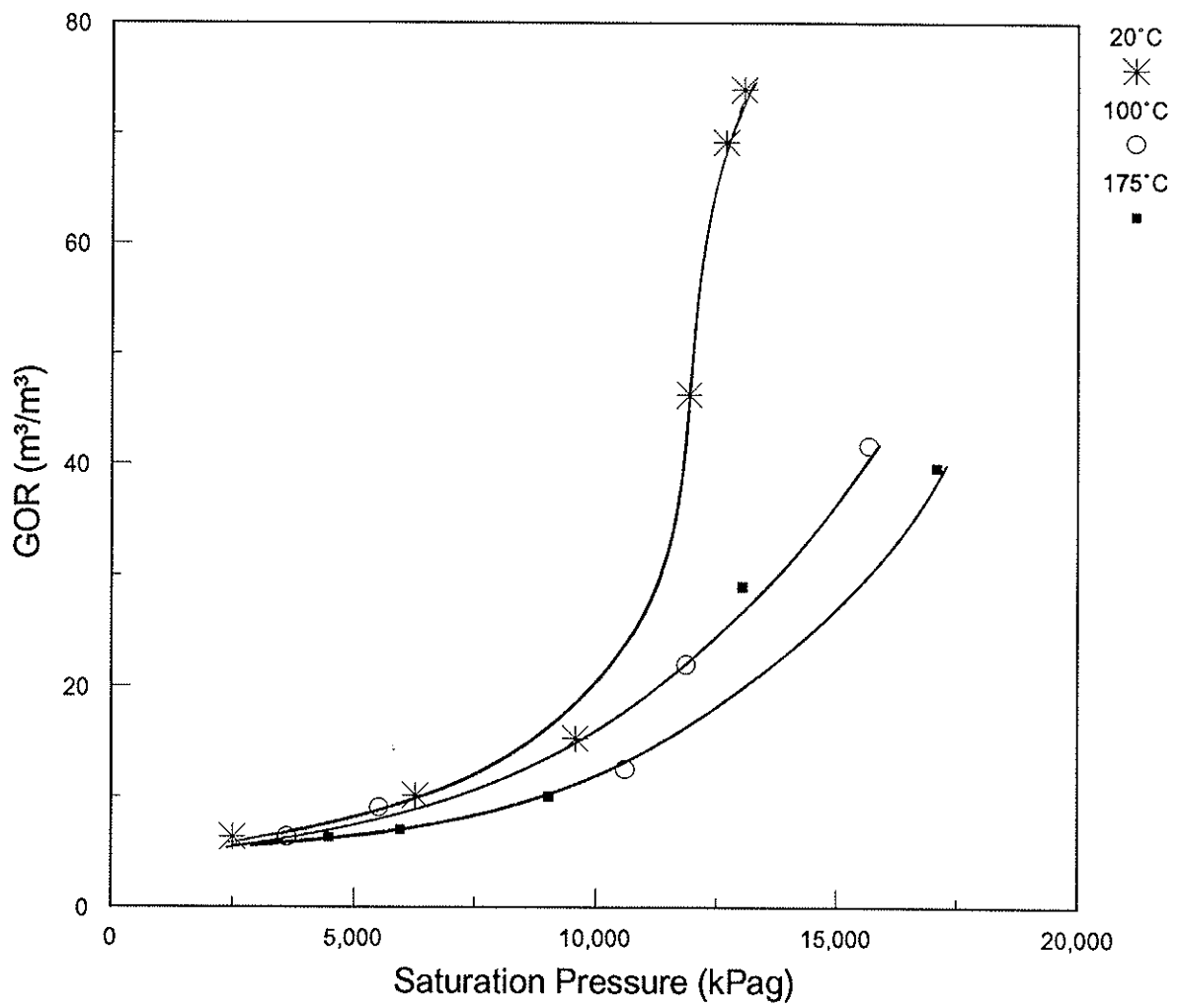
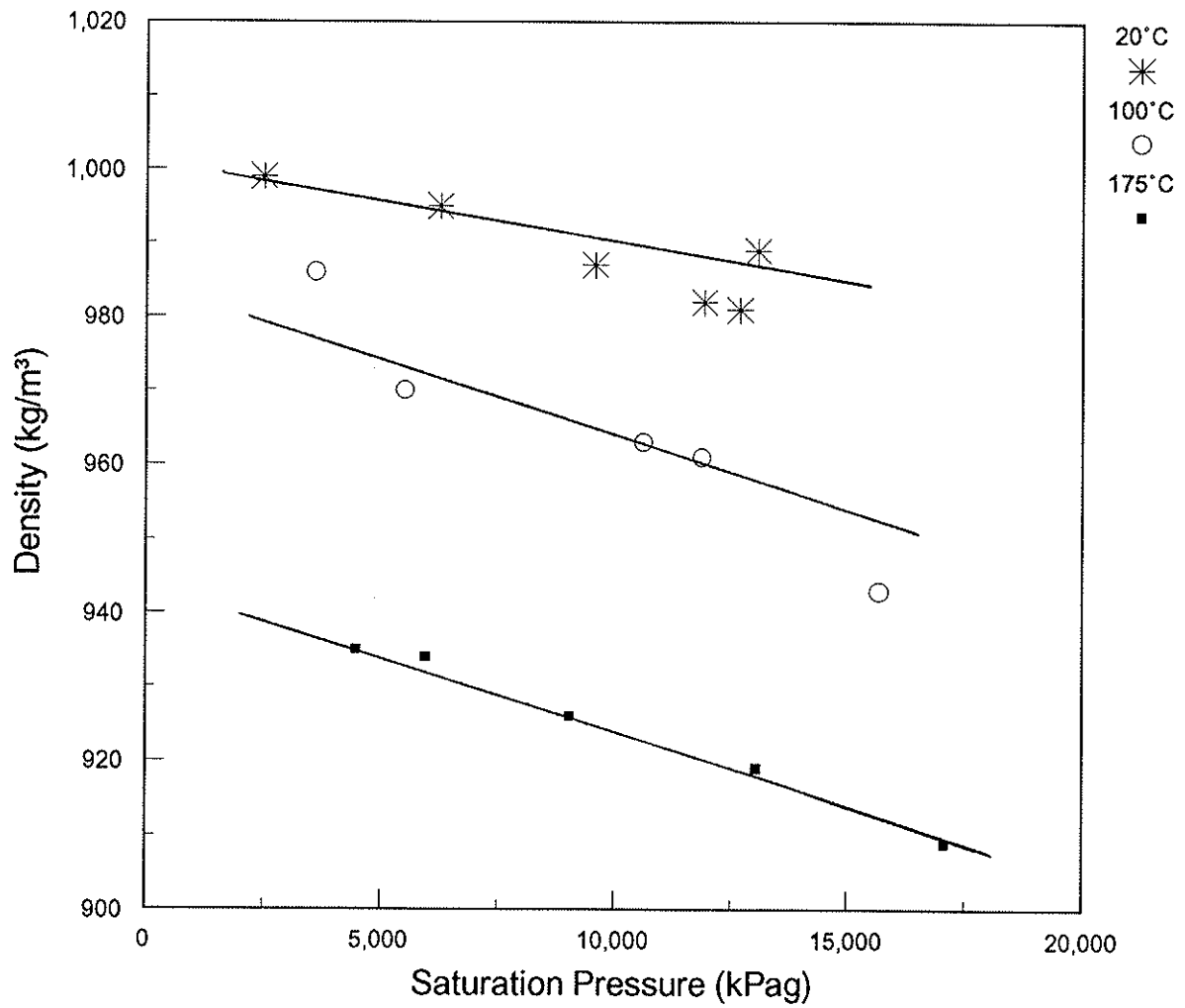


FIGURE 18
MEASURED PHYSICAL PROPERTIES AS A FUNCTION OF CO2 CONCENTRATION
OIL #3 (9.6° API)
DENSITY vs SATURATION PRESSURE



**FIGURE 19
CORE DISPLACEMENT APPARATUS**

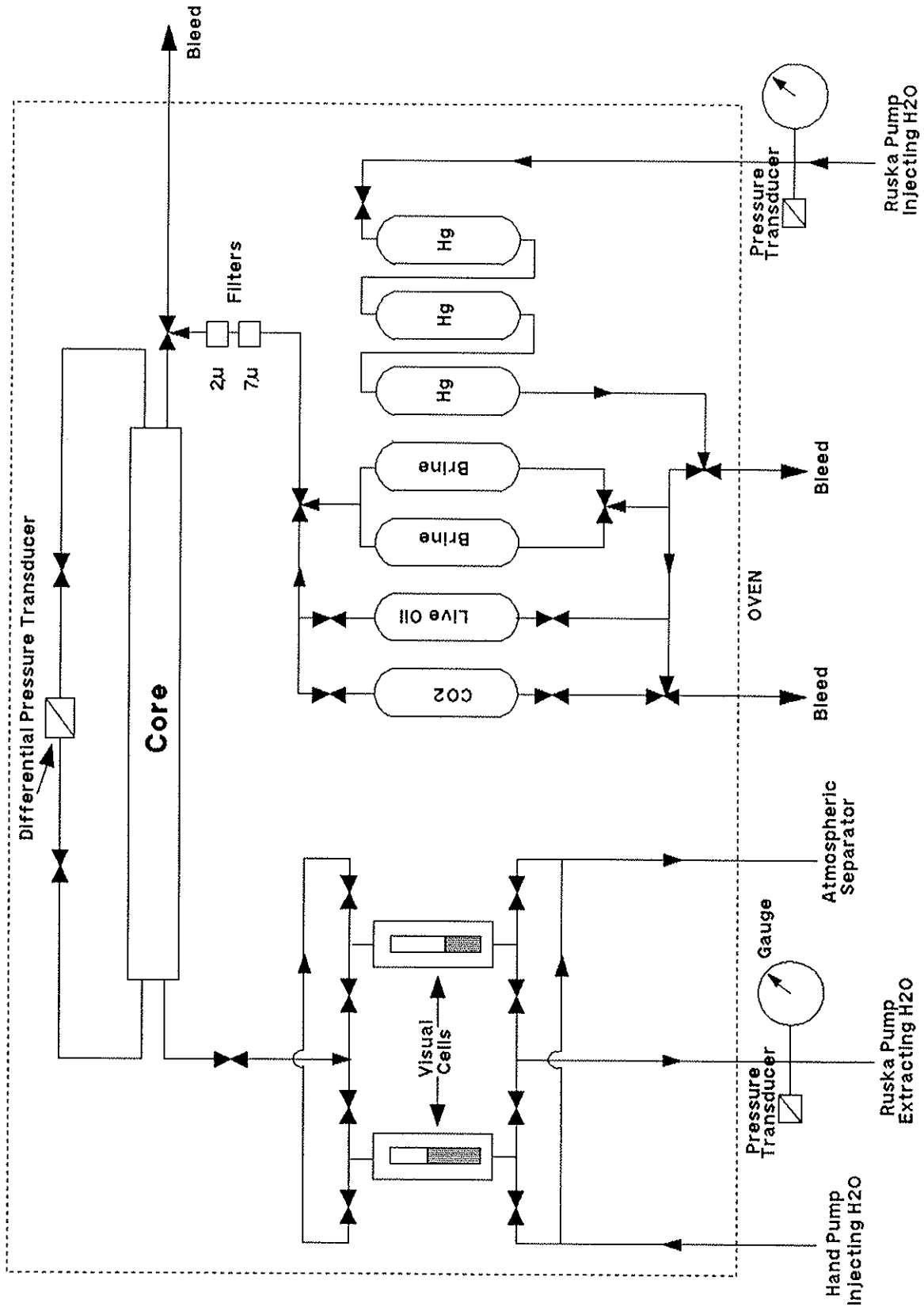
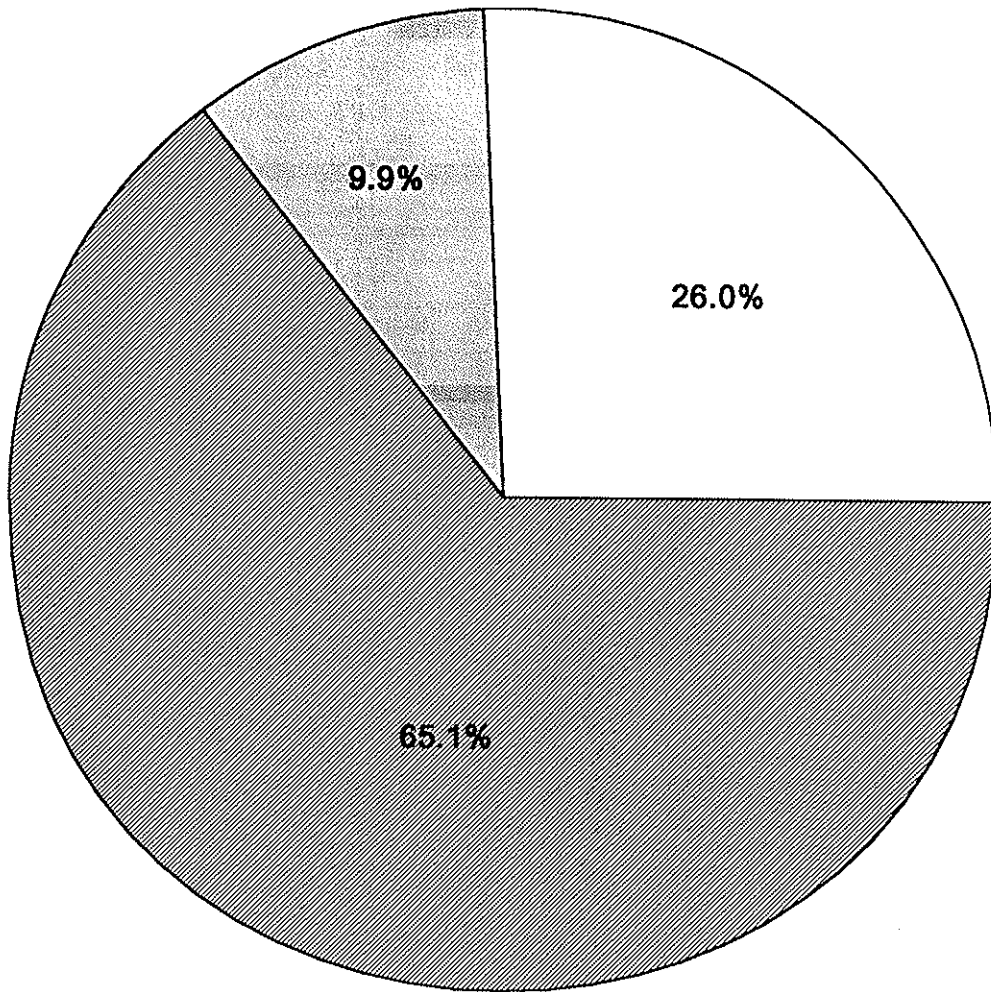


FIGURE 20
FRACTIONAL RECOVERIES FROM COREFLOOD USING
15°API GRAVITY OIL (OIL #1)



Waterflood Recovery

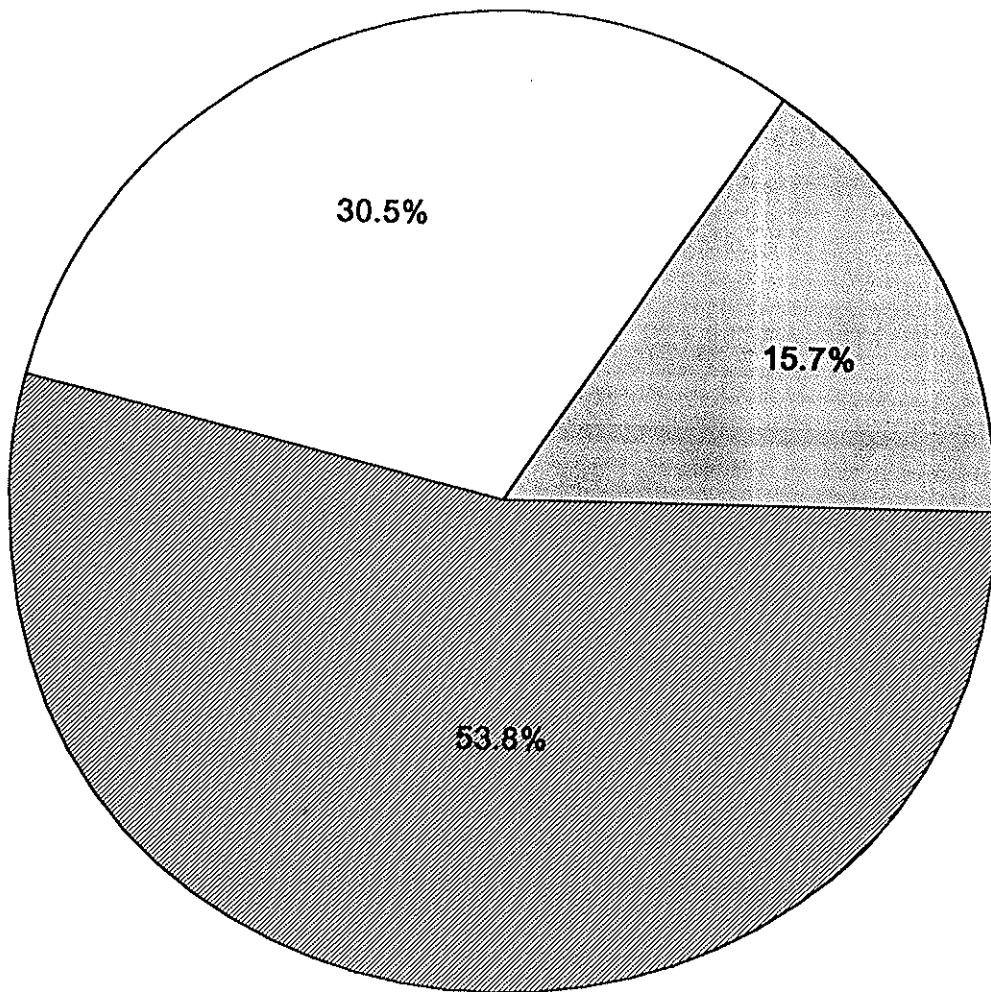


Tertiary Recovery
By Water-CO2 WAG





Unrecovered Oil

FIGURE 21
FRACTIONAL RECOVERIES FROM COREFLOOD USING
12.4°API GRAVITY OIL (OIL #2)



 Waterflood Recovery

 Tertiary Recovery
By Water-CO2 WAG

 Unrecovered Oil

APPENDIX A

Summary of Carbon Dioxide Physical Properties

Molecular Weight	44.01	44.01
Critical Temperature	31.0 °C	87.8 °F
Critical Pressure	7386 kPa	1071 psi
Critical Density	465 kg/m ³	29.0 lb/ft ³
Eccentric Factor	0.225	0.225
Normal Sublimation Temperature (1)	-78.5 °C	-109.3 °F
Triple Point Temperature	-56.5 °C	-69.9 °F
Triple Point Pressure	517.8 kPa	75.1 psia
Density of Solid @ (-78.5° C) (1)	1565 kg/m ³	97.7 lb/ft ³
Density of Liquid @ (0° C, 4 MPa)	915 kg/m ³	57.1 lb/ft ³
@ (-35° C, 2 MPa)	1095 kg/m ³	68.4 lb/ft ³
Density of Gas @ (15° C), (1)	1.872 kg/m ³	0.1169 lb/ft ³
Latent Heat of Fusion @ T.P.	198 kJ/kg	85 Btu/lb
Latent Heat of Sublimation @ (-78.5° C) (1)	572 kJ/kg	246 Btu/lb
@ T.P.	543 kJ/kg	234 Btu/lb
Latent Heat of Vaporization @ T.P.	348 kJ/kg	150 Btu/lb
@ (0° C)	234 kJ/kg	101 Btu/lb
@ (20° C)	155 kJ/kg	66.7 Btu/lb
Specific Heat of Solid (-79° C to 20° C)	1.45 kJ/kg K	0.346 Btu/lb° F
Specific Heat of Liquid (below -15° C)	1.90 kJ/kg K	0.46 Btu/lb° F
Specific Heat of Gas (1), Cp, (-79° C to -15° C)	0.79 kJ/kg K	0.190 Btu/lb° F
Cp, (-15° C to 20° C)	0.83 kJ/kg K	0.198 Btu/lb° F
Cv, (-79° C to -15° C)	0.58 kJ/kg K	0.143 Btu/lb° F
Cv, (-15° C to 20° C)	0.63 kJ/kg K	0.151 Btu/lb° F
Thermal conductivity of Liquid @ (-20° C)	0.190 W/m K	0.109 Btu/ft h °F
@ (+20° C)	0.092 W/m K	0.053 Btu/ft h °F
Thermal Conductivity of Gas (1) @ (0° C)	0.0143 W/m K	0.0083 Btu/ft h °F
@ (30° C)	0.0166 W/m K	0.0096 Btu/ft h °F
Viscosity of Gas @ (15° C) (1)	0.015 cP	0.015 cP
Viscosity of Liquid @ (-20° C, 2 MPa)	0.14 cP	0.14 cP
(1) @ 101.325 kPa		